

# Chemical composition of surface- and groundwater in fast-weathering silicate rocks in the Seiland Igneous Province, North Norway

Ingrid Stober<sup>1</sup>, Holger Teiber<sup>2</sup>, Xiaoyan Li<sup>2</sup>, Natalie Jendryszczyk<sup>2</sup> & Kurt Bucher<sup>2</sup>

<sup>1</sup>Karlsruhe Institute of Technology (KIT), Institute of Applied Geosciences (AGW), Adenauerring 20B, Bld. 50.40, D-76131 Karlsruhe, Germany.

<sup>2</sup>University of Freiburg, Mineralogy & Petrology, Albertstr. 20B, D-79102 Freiburg, Germany.

E-mail corresponding author (Ingrid Stober): [ingrid.stober@kit.edu](mailto:ingrid.stober@kit.edu).

The geochemical composition of nepheline-syenite, carbonatite, ultramafic rocks and gabbro samples from the Seiland Igneous Province is presented in terms of whole-rock chemistry, major and selected trace elements, and mineralogy. Additionally, the hydrochemistry of around 100 surface water, groundwater, rainfall and seawater samples from the area is presented. Surface water and groundwater solute chemistry can be explained in terms of reaction of precipitation with bedrock minerals: the waters thus acquire a clear chemical signature dependent on the catchment's lithology. The mineralisation of the waters (total dissolved solids or TDS) is generally low, although it is somewhat elevated in carbonatite- or nepheline-syenite-dominated terrains, in comparison with ultramafic, gabbro or granitic terrains. Additionally, each lithology exhibits its specific water type. Thus, waters in a nepheline-syenite-dominated terrain tend to be Ca-Na-HCO<sub>3</sub> rich with relatively high pH, whereas waters in carbonatite terrains are Ca-HCO<sub>3</sub> dominated with only slightly elevated pH. Waters in ultramafic rocks exhibit strongly elevated Mg concentrations with circumneutral pH, whereas waters from gabbros are variable in terms of their major cation (Mg, Ca, Na) composition. Mineral stability diagrams aid our understanding of the evolution of rainwater by chemical interaction with rocks in each lithology. In gabbro and ultramafic terrains, such diagrams suggest that kaolinite is likely to be the primary alteration product and that saturation with respect to calcite will not be reached; instead, the waters will evolve until saturation with respect to stilbite (a Na-Ca zeolite mineral) is attained. Waters in ultramafic rocks will then follow this stable phase boundary until saturation with respect to chlorite is achieved. The gabbro waters, on the other hand, could also follow the stable phase-boundary to stilbite until saturation with respect to paragonite (a sodium mica) is reached, depending on the plagioclase-to-clinopyroxene ratio (Plg/Cpx). Surprisingly, it is found that olivine (i.e., forsterite) does not control the water chemistry in gabbros and ultramafic rocks..

*Keywords:* Seiland Igneous Province, hydrochemistry, surface water, groundwater, geochemistry, nepheline-syenite mine

Received 15. January 2017 / Accepted 19. April 2017 / Published online 16. June 2017

## Introduction

The overall motivation of this investigation has been to get a better understanding of the chemical evolution of surface water and groundwater in fractured crystalline bedrocks. Solutes and gases in surface water and groundwater can derive from many different sources. Main contributions to the chemical composition include atmospheric input, interaction with the biomass and soil, and mixing with deeper, mineralised groundwater,

dissolution of minerals from bedrock and anthropogenic input (Garrels & Mackenzie, 1971; Raiswell, 1984; Drever & Hurcomb, 1986; Tranter et al., 1993; Brown et al., 1994; Aquilina et al., 1997; Stober et al., 1999). Separation of the different contributions is difficult in densely populated low-altitude catchments covered by vegetation (Hilberg & Riepler, 2016).

In this study, the composition of surface water and groundwater under arctic climate conditions in a barely populated area with a thin or deficient biomass and

Stober, I., Teiber, H., Li, X., Jendryszczyk, N. & Bucher, K. 2017: Chemical composition of surface- and groundwater in fast-weathering silicate rocks in the Seiland Igneous Province, North Norway. *Norwegian Journal of Geology* 97, 63–93. <https://dx.doi.org/10.17850/njg97-1-04>.

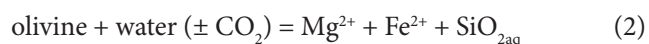
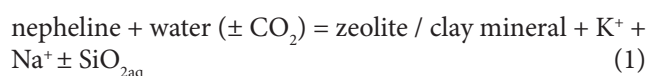
© Copyright the authors.

This work is licensed under a Creative Commons Attribution 4.0 International License.

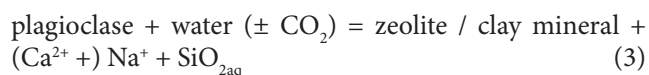
soil cover is investigated. In these catchments far north of the Arctic Circle, the diverse potential contributions to the chemical composition of surface water and groundwater are very limited. In more or less bare-rock areas, the chemical weathering of rocks and minerals causes primarily solute acquisition of surface waters. Thus, the chemical reaction of atmospheric precipitation with exposed fractured rocks is the main cause for the observed composition of surface water. Since the area of investigation is surrounded by sea, a marine influence is to be expected.

The Seiland Igneous Province in North Norway has an extremely varied bedrock geology, including nepheline-syenite, carbonatite, gabbro and ultramafic rocks (e.g., Heier, 1961; Bennett, 1974; Bruland, 1980; Gardner, 1980; Strand, 1981; Robins, 1996; Gautneb, 2009). Since these rocks are composed of relative fast-weathering minerals compared with granites or gneisses, this diverse bedrock geology is expected to be reflected in the composition of waters in the brooks and lakes of the investigation area.

Additionally, by studying the process of faster weathering minerals like nepheline or olivine (eq. 1, 2, detailed chemical formulas: eq. 6, 11), it was expected to gain a better general insight into the kinetics of the weathering-reaction of silicate rocks:



The fundamental water-rock interaction (WRI), i.e., the alteration/weathering of common crystalline basement rocks like granites and gneisses (eq. 3, detailed chemical formula: eq. 8; Bucher & Stober, 2000, 2001), is difficult to observe directly in nature because of the slow reaction of this process (Frengstad, 2002; Banks & Frengstad, 2006; Frengstad & Banks, 2007), especially in anorthite (An)-poor plagioclase.



Thus, the model process of faster weathering minerals should help us to gain a better insight into the alteration processes of crystalline rocks with slower weathering components.

On the island Stjernøya of the Seiland Igneous Province in northern Norway (Fig. 1), there is a huge outcrop of a nepheline-syenite body with one of the largest (sub) surface nepheline mines in the world (e.g., Heier, 1961; Bruland, 1980; Robins, 1996; Roberts, 2007). In the nepheline-syenites, relatively fast reaction kinetics were to be expected, to observe directly the development of the hydrochemical properties of waters due to alteration processes (WRI). To collect water and rock samples

within the nepheline-syenite mine, run by Northcape Minerals AS, was a unique possibility. By reason of the mine's vertical depth extension of about 700 m, it is possible to study the influence of increasing depth, e.g., prolonged reaction time, extended contact surfaces, etc., on the hydrochemistry of waters. Analogue studies in the likewise 700 m-deep Clara mine, situated in gneisses of the Black Forest (southwest Germany), showed increasing solutes and a change in water type with increasing depth (Stober et al., 2002). Thus, hydrochemistry, flow path, contact time, and geochemistry of the rock and alteration products provide insight into total reaction rates (e.g., Anderson, 1996; Drever, 1997). By studying the weathering process of nepheline-syenite it was expected to deduce a model for water-rock interaction (WRI) in aluminium-silicate rocks.

Another reference system to study relatively fast weathering rocks relates to the presence of carbonatites, which occur in surface outcrops in close proximity to the mine on Stjernøya (Bruland, 1980; Strand, 1981; Gautneb, 2009). In the carbonatite, calcite is the only carbonate phase. Calcite is a very fast weathering mineral.

Olivine, present in ultramafic rocks and in olivine-gabbros of the Seiland Igneous Province, also weathers at a very fast rate compared to other Mg-Fe-silicate minerals, such as hornblende and mica (Lasaga, 1984, 1998). The alteration process of olivine (eq. 2) and its influence on hydrochemistry is considered to be very important. The intention was to find out if this process can be regarded as a model for Fe-Mg-silicates or if there are other minerals controlling the weathering process more decisively. In olivine-free or -poor gabbro catchments, the weathering process of pyroxene and plagioclase is expected to have a dominant control of the chemical properties of these waters.

Thus, the overall aim and motivation of the study has been to better understand the chemical evolution of surface water and shallow groundwater in fractured aluminium-silicate rocks. All the investigated rock-types in the Seiland Igneous Province, i.e., nepheline-syenite, carbonatite, gabbro and ultramafic rocks, are exposed to more or less identical hydrological conditions, which makes the island uniquely suited for investigations on weathering effects in different fractured, crystalline bedrocks. The study is mainly focused on surface waters with a relatively short contact time in the rocks. Nevertheless, investigations in the 700 m-deep underground mine on Stjernøya and in two tunnels (through gabbro and granite) were carried out to see how the infiltrating water chemistry evolves with depth.

In contrast to this study, Pfeifer (1977), Clark & Fontes (1990), Marques et al. (2008), Chavagnac et al. (2013) and Miller et al. (2016) investigated upwelling springs deriving from ultramafic rocks. The spring waters showed high TDS and pH values. According to Marques

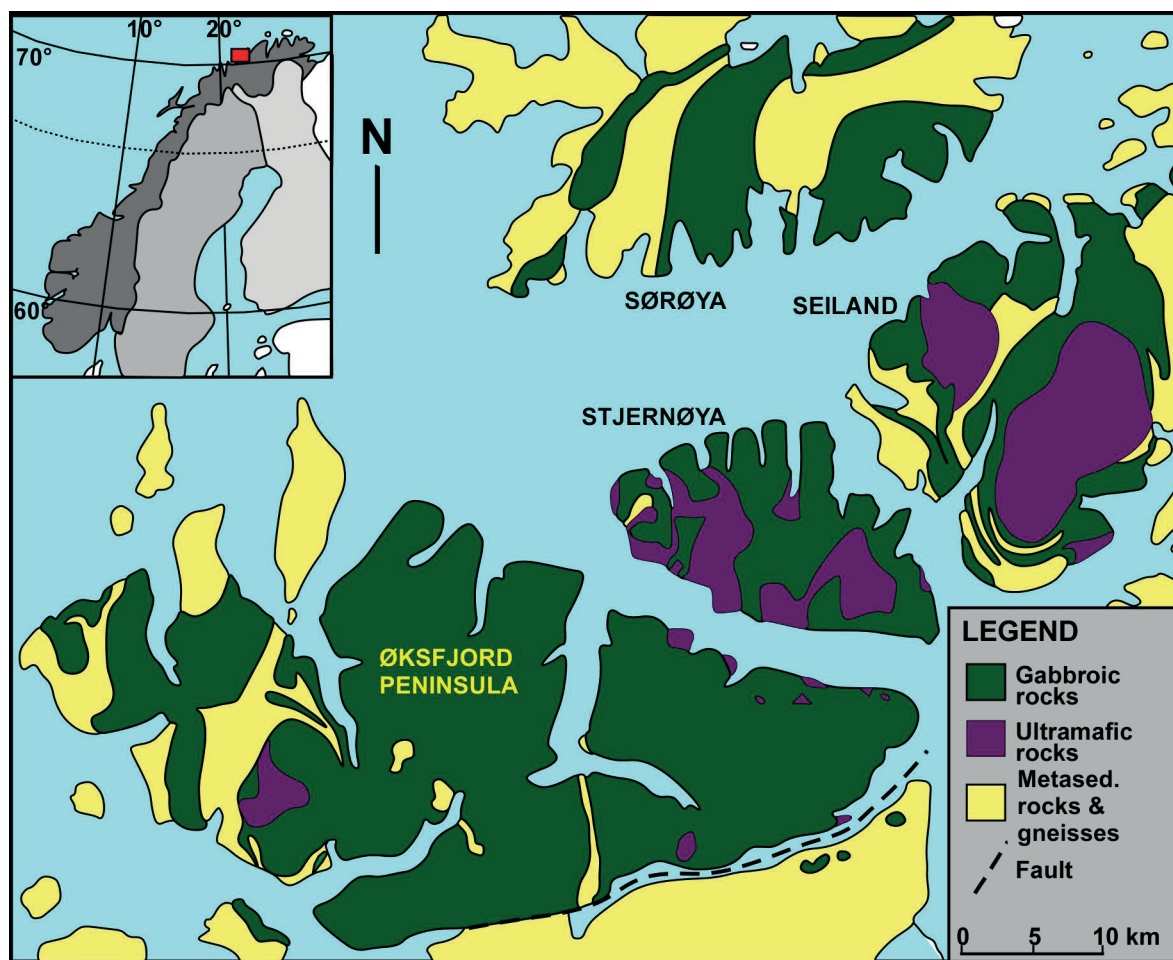


Figure 1. Schematic geological map of the Seiland Igneous Province in Finnmark, North Norway (after Griffin et al., 2013).

et al. (2008), these waters belong to a Ca–OH water type, most probably depleted in Mg as a result of precipitation of brucite and serpentine minerals at the surface.

Investigations on surface waters in ultramafic rock and/or gabbro catchments have been carried out by, e.g., Barnes & O’Neil (1969), Barnes et al. (1978), Clark & Fontes (1990), Gascogne & Kamieni (1993), Drever (1997), Venturelli et al. (1997), Zedef et al. (2000), Zakharova et al. (2007), Zhou (2010), Chavagnac et al. (2013) and Bucher et al. (2015). Typical waters from ultramafic rock terrains are Mg–HCO<sub>3</sub> type waters with elevated pH values.

In contrast to this study, most of the above investigations were not focused on a detailed development of rainwater in contact with relatively fast-weathering crystalline basement rocks. Additionally, most examinations were carried out in the so-called Temperate Zone, i.e., under moderate temperature conditions, in most cases even under Mediterranean climatic conditions, whereas our research has been done in the Polar Regions, i.e., under arctic climate conditions.

To our knowledge, investigations on how water will evolve in carbonatite- or nepheline-syenite terrains under these climatic conditions have not previously been carried out in detail. However, Zakharova et al. (2007) described the composition of groundwater in the Karelia region and the Kola Peninsula, NW Russia, and linked it to that of the bedrock, but no detailed investigations were carried out describing the weathering process and the evolution of the waters. Either way, the total of solutes (TDS) in these areas of NW Russia are in the same order of magnitude as the water samples collected by us in the Seiland Igneous Province.

This paper also presents the first systemic investigation of the hydrochemical properties of surface waters in the different rock-types of the Seiland Igneous Province, i.e., nepheline-syenite, carbonatite, gabbro and ultramafic rocks.

## Topography, hydrology and geology of the investigated area

The Seiland Igneous Province consists of a deep-seated alkaline magmatic suite of dominantly gabbroic composition and is located in the county of Finnmark, northern Norway, and hosted within the northernmost part of the Caledonian orogenic belt (Fig. 1). The island Seiland lies more or less in the centre of this igneous province, surrounded by Sørøya, Stjernøya and the Øksfjord Peninsula.

Situated far north of the Arctic Circle at latitude of 70° N, for two months of the winter the sun is always below the horizon. Correspondingly, during the summer the county benefits from two months of midnight sun. The topography of the Seiland Igneous Province is very rough with steep mountain sides down to the sea and peaks up to about 1.000 m a.s.l. The coast is indented by large fjords and the whole area is more or less above the treeline with stunted birch in sheltered fjord areas. The central parts of the islands are glaciated, in part with huge plateau glaciers like the Øksfjordjøkelen (45 km<sup>2</sup>) or the Seilandsjøkelen (14 km<sup>2</sup>). The Øksfjord plateau glacier calved directly into the sea (Jøkelfjorden) until the last century, but is today slowly receding.

In Finnmark, the Sámi culture is still thriving; especially notable is the reindeer husbandry with summer grazing at the coastal areas and winter grazing on the heathland plateau inland. Due to the mineralogy of the bedrock, soils of the Seiland Igneous Province are generally carbonate-rich. Especially on Stjernøya the soils are rich in carbonate and potassium minerals and are therefore very fertile (Heim et al., 2010). Thus, the island is more or less a green grassland. In summer large flocks of reindeer are now brought by the Sámi to the island for grazing, whereas earlier the reindeer had to swim across the Stjernesund.

Annual precipitation is about 830 mm, with somewhat lower rain- or snowfall in spring and higher in the autumn. Mean annual temperature is about 3.1°C. The area is very sparsely inhabited and the population is steadily declining. Stjernøya, for example, now has no road or ferry connections.

The approximately elliptical Seiland Igneous Province, about 100 km x 50 km in size, consists of different intrusions such as mafic and ultramafic plutons, mafic dykes, alkaline complexes and carbonatite bodies (Bennett, 1974; Roberts et al., 2010). The intrusions were emplaced during a time span from 570 to 520 Ma (Roberts et al., 2006, 2010; Menegon et al., 2011), in an inferred intracontinental rift setting, most likely related to the incipient stages of opening of the Iapetus Ocean (Siedlecka et al., 2004; Roberts et al., 2006; Menegon et al., 2011). Thus, the Seiland Igneous Province is supposed to represent the eroded roots of an intracontinental rift

igneous complex, similar to the East African Rift Valley. The occurrence of nepheline-syenites and carbonatites within the province is one supportive argument (Mjelde, 1983; Kirkland et al., 2008; Roberts et al., 2010). In general, the tectonic evolution of the Seiland Igneous Province and whole of Finnmark is complex and still under discussion.

The Caledonian fold and thrust belt emerged from the collision of the continents Laurentia and Baltica in Silurian times, where the margin of Baltica is considered as having been subducted beneath Laurentia (Torsvik et al., 1996; Roberts, 2003). As a result of this collision a stack of nappes was produced on the Precambrian basement of Baltica. The allochthonous nappes are basically composed of Neoproterozoic to Silurian metasedimentary rocks intruded by diverse igneous bodies and dykes. This overthrust package, consisting of four major nappe complexes, caused crustal thickening and associated metamorphism, similar to the Alpine orogeny (Bucher, 1991). The Seiland Igneous Province occupies the westernmost part of one of these nappes, the Kalak Nappe Complex.

Gabbroic plutons form the dominant element of the Seiland Igneous Province and generally comprise layered bodies ranging in composition from tholeiite to alkali olivine gabbro, and locally grading into diorite and monzonite (Bennett, 1974; Gardner, 1980; Tegner et al., 1999). Ultramafic intrusions are variable in size and are unzoned (Figs. 1 & 2). They have cut the mafic plutons during their intrusion and consist mainly of olivine clinopyroxenite. Several alkaline complexes comprise primarily hornblende clinopyroxenite, alkali syenite, carbonatite and nepheline-syenite (Oosterom, 1963; Sturt & Ramsay, 1965; Robins, 1971, 1972, 1996; Robins & Gardner, 1975; Robins & Tysseiland, 1983; Roberts et al., 2010).

Globally, nepheline-syenite and carbonatite are relatively uncommon rocks; however, in the Seiland Igneous Province they are comparatively widespread as large complexes. One of the best known carbonatitic bodies is located NNE of Lillebukt in the south of Stjernøya forming the northern slope of the mountain Nabbaren, where the nepheline-syenite is mined by Northcape Minerals, and is extending to Smaldalen in the north. In addition, nepheline-syenite dykes are found throughout the Seiland Igneous Province. Syenite rocks, carbonatites and mafic dykes are the youngest igneous rocks in the province and are believed to be related to the nephelinitic magmatism. The nepheline-syenite pegmatites represent the latest phase of magmatic activity at c. 520 Ma (Pedersen et al., 1989) and are thus older than the Caledonian orogeny.

The Lillebukt Alkaline Complex covers a 13 km<sup>2</sup> area situated in the south of the island Stjernøya. It is dominated by syenite, nepheline-syenite, apatite-

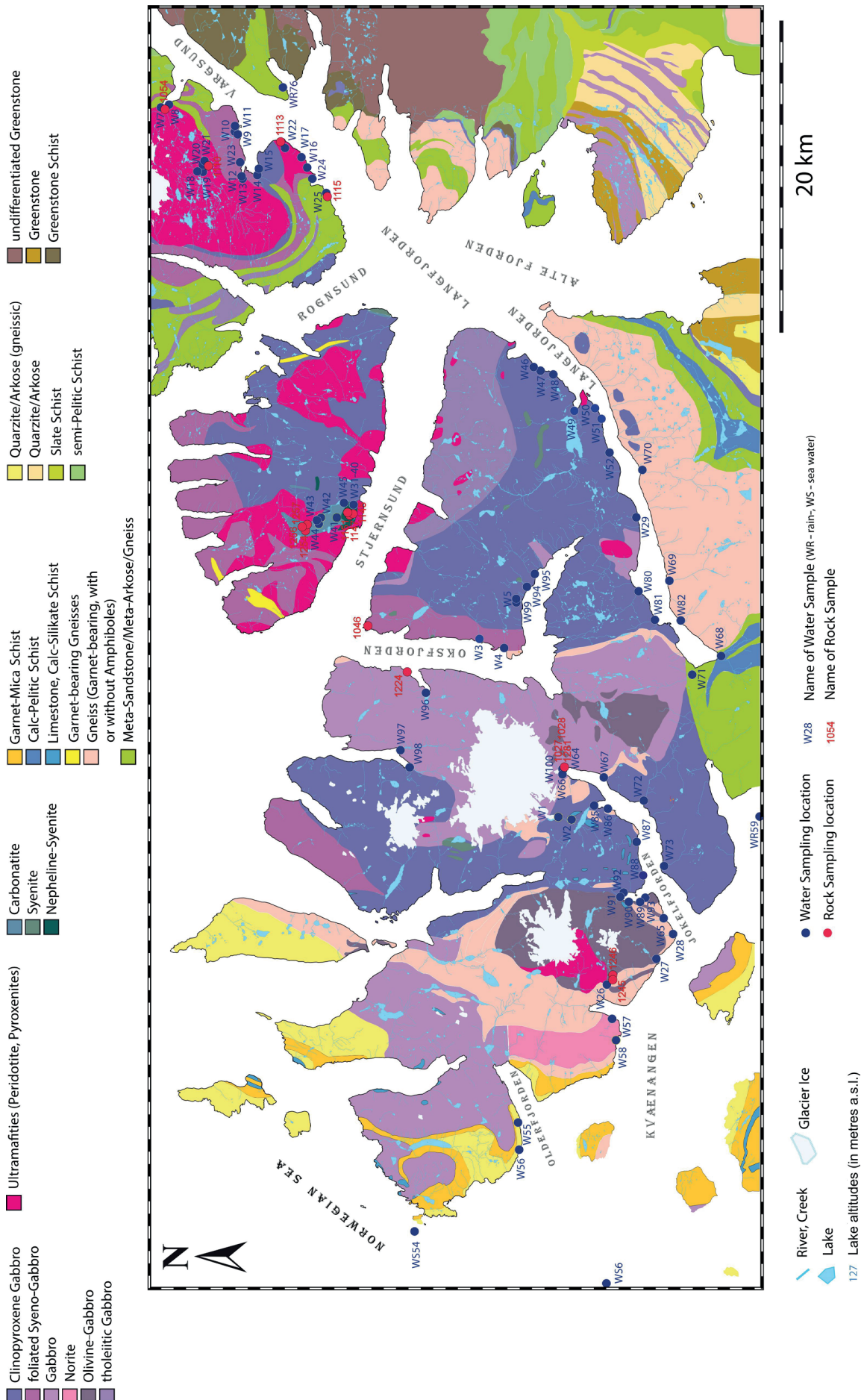


Figure 2. Geological map of the Seiland Igneous Province showing all water and selected rock sample sites (after Roberts, 1973).

Table 1. Major and selected trace elements of rocks in the Seiland Igneous Province.

Sample #	1246	1027	1046	1028	1054	1224	1281	1115	1245	1110	1113	1254	1256	1257	1147	1145	1151
Geology	Gabbro, olivine-gabbro	Gabbro, anorthosite	Gabbro, olivine-gabbro	Gabbro, olivine-gabbro	Gabbro, olivine-gabbro	Gabbro, troctolite	Gabbro, olivine-gabbro	Gabbro, olivine-gabbro	Gabbro, olivine-gabbro	Peridotite, ultramafic rock	Peridotite, ultramafic rock	Carbonatite	Carbonatite	Carbonatite	Nephelin-syenite	Nephelin-syenite	Nephelin-syenite
Major elements [wt.%]																	
SiO <sub>2</sub>	50.43	50.75	40.55	46.95	47.56	45.62	44.13	45.62	49.39	39.47	39.52	23.19	28.97	25.98	53.87	54.36	53.31
TiO <sub>2</sub>	0.76	0.35	3.74	0.76	1.04	3.79	0.63	1.32	1.26	0.40	0.28	3.79	2.84	3.67	0.35	0.27	0.50
Al <sub>2</sub> O <sub>3</sub>	14.96	26.48	22.00	14.95	19.34	18.81	8.82	11.40	6.31	2.79	2.76	8.44	14.69	8.95	24.00	24.07	23.11
Fe <sub>2</sub> O <sub>3</sub> <sup>tot</sup>	7.14	2.59	9.81	6.91	7.08	12.71	13.82	13.40	9.76	13.30	12.54	14.38*	11.51*	16.66*	2.24	1.85	2.95
MnO	0.13	0.04	0.10	0.12	0.12	0.15	0.24	0.19	0.17	0.19	0.18	0.41	0.32	0.42	0.05	0.03	0.06
MgO	11.33	2.51	6.44	12.26	7.43	5.81	22.23	16.49	14.84	32.20	34.27	2.95	2.06	3.84	0.08	0.04	0.14
CaO	12.90	12.73	12.47	15.17	12.60	8.43	9.78	9.42	17.70	6.34	4.70	20.72	16.66	17.54	1.79	1.52	2.69
Na <sub>2</sub> O	1.80	3.67	2.26	1.52	3.20	3.57	1.00	1.80	0.71	0.27	0.29	1.55	4.70	1.86	7.46	7.82	7.32
K <sub>2</sub> O	0.20	0.23	0.57	0.13	0.61	0.55	0.16	0.45	0.03	0.03	0.06	3.85	2.16	3.01	8.66	8.06	8.43
P <sub>2</sub> O <sub>5</sub>	0.04	0.03	0.05	0.02	0.22	0.23	0.04	0.16	0.02	0.02	0.04	1.40	0.84	1.40	0.04	0.03	0.06
SUM	99.69	99.38	97.99	98.79	99.20	99.67	100.85	100.25	100.19	95.01	94.64	66.30	73.24	66.67	98.07	97.05	97.94
LOI [wt.%]	0.96	1.28	2.83	1.84	1.28	0.55	0.22	1.57	0.40	6.95	6.46	16.18	10.83	11.41	1.01	1.50	1.08
Selected trace elements [ppm]																	
Cr	475	45	<10	1178	42	54	2197	1056	827	1829	2255				55	10	94
Co	44	14	43	44	33	39	90	77	54	107	116				1	-	1
Ni	176	20	50	161	100	32	493	478	241	1025	1147				6	5	6
Cu	76	16	49	19	62	37	33	49	141	29	163	33	22	37			
Zn	52	14	46	34	44	100	109	96	55	72	59	199	135	227	13	13	16
Sr	507	975	1091	404	894	1011	209	276	102	30	47	4921	5702	4362	2712	2331	2488
Zr	38	21	53	39	87	142	76	92	59	27	24	163	150	287	36	27	52
Ba	76	174	260	30	291	432	50	125	<10	4	15	2729	3091	5840	1809	1858	1515

\*FeO

rich hornblende-clinopyroxenite dykes, hornblendite, metagabbro and silicocarbonatite and can be regarded as an irregularly deformed and metamorphosed ring-complex with the carbonatite as the latest intrusion (Skogen, 1980). The central part of the silicocarbonatite intrusion is dominated by biotite. Along the margin of the carbonatites, there are many apatite-rich hornblende-clinopyroxenite dykes which are surrounded by fenites and are believed to represent injections from an olivine melanephelinite magma undergoing fractional crystallisation (Strand, 1951; Heier, 1961; Bruland, 1980; Mjelde, 1983; Robins, 1996).

## Sampling and analytical methods

### General information

Overall, an extensive and broad collection of rock and water samples from the Seiland Igneous Province was carried out during fieldwork in the summers of 2003 and 2009. Fig. 2 shows the localities of all collected

water samples and of selected rock samples, important within this context. Sampling was carried out mainly on the islands of Stjernøya, Seiland and on the Øksfjord Peninsula and was achieved by using a small motor-boat to gain access and to collect samples in the different lithological units. Care was taken to acquire representative rock samples of each lithological unit and to obtain water samples from the different but well defined catchment basins with equal lithological units, in order to obtain general information on the surface-water composition dependent on the varying geology. Water and rock samples were also taken from inside the nepheline-syenite mine of Northcape Minerals, i.e., within the mountain Nabbaren on Stjernøya, and in two tunnels, Stetind- and Øksfjordtunnel, beneath overlying ground reaching up to about 1000 m and 350 m, respectively.

Information concerning the rock- and water samples is listed in Tables 1 & 2A–E, together with the major- and trace-element geochemistry of the rock samples (Table 1) and the hydrochemical results of the water samples (Table 2A–E).

**Table 2A.** Hydrochemical analyses of sea-water and rainfall samples. For standard ocean water see: [www.lenntech.com/composition-seawater.htm](http://www.lenntech.com/composition-seawater.htm).

Sample	WS6	WS54	Standard	WR59	WR76
Location	Sea water	Sea water	Ocean water	Rainfall	Rainfall
Date	17. Jul. 03	14. Aug. 03	-	13. Aug. 03	15. Aug. 09
Temp. (°C)	18.0	16.6	-	16.7	nd
pH	8.18	8.20	7.5–8.4	4.64	nd
Redox pot. (mV)	nd	nd	-	170	nd
EC (µS/cm) Lab.	nd	nd	-	17.5	nd
<b>Concentration (mg L<sup>-1</sup>)</b>					
Ca	361	359	400	0.32	0.70
Mg	1034	1090	1262	0.10	0.21
Na	8670	9180	10556	1.12	1.11
K	300	327	380	0.49	0.21
Sr	6.53	6.92	13	bd	bd
NH <sub>4</sub>	nd	nd	-	0.32	bd
CO <sub>3</sub>	-	-	-	-	-
HCO <sub>3</sub>	128.75	128.75	140	2.30	1.26
SO <sub>4</sub>	2350	2400	2649	0.90	0.90
Cl	16773	17539	18980	1.38	2.13
HPO <sub>4</sub>	nd	nd	-	bd	bd
NO <sub>3</sub>	nd	nd	-	0.26	0.39
F	1.26	1.26	1	bd	bd
Br	61.50	62.50	65	bd	bd
TDS	29686	31094	34483	7.19	6.91
Br	0.03	bd	0.03	bd	bd
TDS	109.89	75.42	60.51	58.99	54.04

Abbreviations: nd – not determined, bd – below detection limit.

Table 2B. Hydrochemical analyses of water samples collected in the nepheline-syenite mine and in nearby carbonatite-dominated terrain on the island Stjernøya of the Seiland Igneous Province.

Sample	W31	W32	W33	W34	W35	W36	W37	W38	W39	W40	W41	W42	W43	W44	W45
<b>Geology</b>	Neph.-syen. mine	Carbonatite	Carbonatite	Carbonatite	Neph.-syen. & some carbonatite										
<b>Depth (m.a.s.s.)</b>	600	475	320	320	250	250	250	240	500	500	0				
<b>Location</b>	Fissure water	Borehole	Fissure water	Dripping water	Borehole	Borehole	Borehole	Dripping water	Duct	Duct	Spring	Brook	Brook	Brook	Brook
<b>Date</b>	03. Aug. 03	07. Aug. 03	07. Aug. 03	07. Aug. 03	07. Aug. 03	07. Aug. 03									
<b>Temp. (°C)</b>	6.0	6.0	6.0	6.0	6.0	6.0	6.0	6.0	6.0	6.0	12.0	10.0	11.0	12.0	9.0
<b>pH</b>	8.91	9.34	9.36	9.16	9.21	9.36	9.07	7.48	8.21	8.05	8.65	7.97	8.05	7.72	7.87
<b>Redox pot. (mV)</b>	-40	-69	-69	-58	-59	-61	-43	+32	+5	+14	-20	+16	+9	+22	+16
<b>EC (µS/cm)</b>	155.8	105.8	87.4	83.2	73.9	99.8	99.7	61.5	146	130	60.4	99.4	113.4	131.6	55.8
<b>Lab.</b>															
<b>Concentration (mg L<sup>-1</sup>)</b>															
<b>Ca</b>	7.58	6.24	8.16	7.99	8.35	11.08	10.09	6.09	17.8	17.35	7.11	14.58	17.7	23.45	6.96
<b>Mg</b>	0.41	0.29	0.50	0.37	0.42	0.66	0.51	0.26	0.36	0.46	0.33	0.66	0.77	0.51	0.37
<b>Na</b>	24.57	19.46	6.73	6.70	5.70	6.25	11.15	4.91	13.28	7.77	3.58	4.41	4.82	3.12	3.6
<b>K</b>	1.06	1.40	1.24	0.96	1.00	0.92	1.28	0.86	1.86	1.33	0.45	0.86	1.04	1	0.44
<b>Sr</b>	0.34	bd	0.33	0.43	bd	0.42	0.65	1.21	0.09						
<b>NH<sub>4</sub></b>	bd	bd	bd	bd	bd										
<b>CO<sub>3</sub></b>	3.00	4.80	3.00	1.80	1.80	3.3	1.5	-	-	-	0.9	-	-	-	-
<b>HCO<sub>3</sub></b>	44.54	25.02	15.26	18.31	22.58	13.42	23.8	28.07	58.58	48.82	21.66	53.09	61.02	75.66	26.54
<b>SO<sub>4</sub></b>	17.01	9.67	4.26	3.98	3.24	5.58	6.29	2.45	10.77	10.61	1.42	2.96	3.55	2.64	1.5
<b>Cl</b>	10.52	6.97	5.99	6.32	4.69	7.33	6.32	3.46	4.67	4.44	4.9	3.58	3.94	3.23	3.54
<b>HPO<sub>4</sub></b>	bd	bd	bd	bd	bd										
<b>NO<sub>3</sub></b>	0.80	1.57	15.34	12.56	6.26	17.44	15.09	0.6	10.59	7.24	0.25	0.09	0.12	0.7	bd
<b>F</b>	0.02	bd	bd	bd	bd	bd									
<b>Br</b>	0.03	bd	0.03	bd	bd	0.04	0.02	bd	bd	bd	bd	bd	bd	bd	bd
<b>TDS</b>	109.89	75.42	60.51	58.99	54.04	66.03	76.05	46.7	118.24	98.45	40.6	80.65	93.61	111.52	43.04

Abbreviations: nd – not determined, bd – below detection limit.

Table 2C. Hydrochemical analyses of water samples collected in the gabbro-dominated terrain of the Seiland Igneous Province.

Sample	W3	W4	W14	W27	W29	W47	W48	W49	W50	W52	W64	W65	W66	W67	W71	W72	W73
Geology	Gabbro																
<b>Minor constit.</b>																	
<b>Location</b>	Brook																
<b>Date</b>	16. Jul. 03	16. Jul. 03	23. Jul. 03	31. Jul. 03	01. Aug. 03	09. Aug. 09	09. Aug. 09	09. Aug. 09	11. Aug. 09	12. Aug. 09	12. Aug. 09						
<b>Temp. (°C)</b>	12.0	13.0	7.0	12.0	12.0	7.1	6.8	6.9	7.0	5.9	12.9	18.7	8.0	12.8	11.3	12.6	12.4
<b>pH</b>	6.89	6.88	7.21	7.08	7.08	7.20	7.16	7.19	7.50	6.12	7.17	5.45	6.98	7.77	7.72	7.46	7.39
<b>Redox pot. (mV)</b>	+72	+43	+53	+33	+60	+58	+70	+63	+57	+112	+428	+187	+389	+341	+318	+387	+320
<b>EC (µS/cm) Lab.</b>	30.8	28.1	41.9	25.6	48.6	17.3	25.5	41.2	96.5	87.1	17.0	110.0	7.0	65.0	27.0	31.0	30.0
<b>Concentration (mg L<sup>-1</sup>)</b>																	
<b>Ca</b>	1.48	1.06	2.19	1.73	2.22	0.69	1.20	2.25	7.63	8.50	0.79	1.93	0.45	2.25	2.00	2.35	1.52
<b>Mg</b>	0.54	0.44	1.49	0.72	1.26	0.58	0.78	0.98	4.05	1.42	0.85	0.59	0.30	1.54	0.87	0.76	0.64
<b>Na</b>	2.66	2.72	3.48	2.47	5.28	2.04	2.73	3.69	6.21	7.23	1.11	2.68	0.89	2.26	1.58	2.18	2.74
<b>K</b>	0.13	0.13	0.23	0.16	0.23	0.14	0.17	0.16	0.21	0.20	0.10	0.26	0.09	0.17	0.18	0.19	0.16
<b>Sr</b>	bd																
<b>NH<sub>4</sub></b>	bd																
<b>CO<sub>3</sub></b>	-	-	-	-	-	-	-	-	-	-	-	-	-	-	-	-	-
<b>HCO<sub>3</sub></b>	8.54	7.32	15.26	7.32	16.48	6.10	7.93	9.15	36.61	28.07	7.02	8.54	3.05	15.87	9.76	10.98	5.49
<b>SO<sub>4</sub></b>	1.87	1.73	2.81	2.44	2.50	1.40	1.77	1.96	4.61	8.46	0.94	3.45	0.89	2.06	2.28	1.84	3.61
<b>Cl</b>	3.09	3.14	3.97	3.02	5.30	1.42	2.98	6.70	9.79	7.12	1.27	3.02	0.91	2.57	1.88	2.66	3.58
<b>HPO<sub>4</sub></b>	bd																
<b>NO<sub>3</sub></b>	bd	bd	bd	bd	bd	0.07	bd	bd	0.07	bd	0.05	bd	0.05	0.02	0.03	bd	bd
<b>F</b>	bd	0.07	bd														
<b>Br</b>	bd	0.03	bd														
<b>TDS</b>	18.31	16.54	29.43	17.86	33.27	12.44	17.56	24.89	69.21	61.07	12.13	20.47	6.63	26.74	18.58	20.96	17.74

Abbreviations: nd – not determined, bd – below detection limit.

Table 2C. (continuation). Hydrochemical analyses of water samples collected in the gabbro-dominated terrain of the Seiland Intrusive Complex.

Sample	W80	W81	W85	W86	W87	W88	W89	W90	W91	W92	W93	W94	W95	W96	W97	W98	W1
<b>Geology</b>	Gabbro																
<b>Minor constit.</b>																	
<b>Location</b>	Brook	River	River	River	Lake												
<b>Date</b>	16. Aug. 09	16. Aug. 09	19. Aug. 09	19. Aug. 09	19. Aug. 09	19. Aug. 09	23. Aug. 09	24. Aug. 09	24. Aug. 09	25. Aug. 09	25. Aug. 09	25. Aug. 09	14. Jul. 03				
<b>Temp. (°C)</b>	22.2	22.9	10.4	9.5	7.9	21.3	19.9	21.4	21.7	22.1	21.3	21.9	22.2	21.7	22.0	22.9	2.0
<b>pH</b>	7.33	6.86	7.23	7.47	7.80	7.73	6.69	6.92	6.93	7.37	7.37	7.09	7.32	6.89	7.02	7.04	6.67
<b>Redox pot. (mV)</b>	+397	+405	+403	+410	+382	+400	+398	+397	+397	+389	+381	+373	+373	+400	+390	+382	+94
<b>EC (µS/cm)</b>	44.5	24.4	28.0	41.0	60.0	87.0	22.2	32.5	24.4	50.3	51.3	37.7	42.6	31.5	24.8	36.0	34.5
<b>Lab.</b>																	
<b>Concentration (mg L<sup>-1</sup>)</b>																	
<b>Ca</b>	5.10	1.73	2.27	2.69	7.32	14.10	1.14	1.26	1.12	5.74	4.15	1.73	3.36	3.01	1.20	1.71	1.46
<b>Mg</b>	0.89	0.64	0.54	0.57	0.76	0.89	0.46	0.77	0.96	0.74	1.52	0.92	0.96	1.00	0.84	1.01	0.65
<b>Na</b>	3.30	2.11	2.11	2.90	3.31	4.01	2.31	2.74	2.02	3.32	3.70	3.27	3.81	2.25	1.80	2.05	3.42
<b>K</b>	0.25	0.18	0.17	0.25	0.33	0.44	0.18	0.18	0.11	0.31	0.28	0.15	0.15	0.17	0.15	0.16	0.21
<b>Sr</b>	bd																
<b>NH<sub>4</sub></b>	bd																
<b>CO<sub>3</sub></b>	-	-	-	-	-	-	-	-	-	-	-	-	-	-	-	-	-
<b>HCO<sub>3</sub></b>	16.29	7.93	6.41	10.44	21.54	37.47	4.10	4.85	8.05	20.01	19.47	12.88	14.77	9.89	6.51	10.92	6.71
<b>SO<sub>4</sub></b>	2.24	2.47	1.75	2.40	4.32	5.28	1.72	3.95	2.21	3.62	4.02	2.52	3.40	4.40	1.82	1.89	1.68
<b>Cl</b>	4.69	2.78	3.43	3.28	4.20	6.50	3.43	3.13	2.72	3.97	4.21	3.81	4.43	2.65	2.36	2.59	6.02
<b>HPO<sub>4</sub></b>	bd																
<b>NO<sub>3</sub></b>	bd	0.02	bd	bd	0.09	0.04	bd	bd	bd	bd	0.03	bd	bd	bd	bd	bd	bd
<b>F</b>	0.02	bd	0.02	bd	bd	bd	bd	bd									
<b>Br</b>	bd	0.02	bd	0.03													
<b>TDS</b>	32.78	17.86	16.68	22.53	41.87	68.73	13.34	16.88	17.21	37.71	37.38	25.30	30.88	23.37	14.68	20.33	20.18

Abbreviations: nd – not determined, bd – below detection limit.

Table 2C (continuation). Hydrochemical analyses of water samples collected in the gabbro-dominated terrain of the Seiland Intrusive Complex.

Sample	W28	W46	W2	W15	W55	W56	W100	W51	W5	W99	W57	W58	W25	W75	W77	W24
<b>Geology</b>	Gabbro	Gabbro	Gabbro	Gabbro	Gabbro	Gabbro	Gabbro	Gabbro	Gabbro	Gabbro	Norite	Norite	Gabbro, gneis	Gabbro calcite	Gabbro calcite	Gabbro, neph-,cye
<b>Minor constit.</b>																
<b>Location</b>	Waterfall	Waterfall	Spring	Spring, talus	Spring, talus	Spring, talus	Large spring	Fracture water	Tunnel, drops	Tunnel, drops	Brook	Brook	Brook	Brook	Brook	Spring, talus
<b>Date</b>	31. Jul. 03	09. Aug. 03	14. Jul. 03	23. Jul. 03	14. Aug. 03	14. Aug. 03	05. Sep. 09	09. Aug. 03	16. Jul. 03	25. Aug. 09	14. Aug. 03	14. Aug. 03	28. Jul. 03	14. Aug. 09	15. Aug. 09	28. Jul. 03
<b>Temp. (°C)</b>	16.0	7.1	3.0	15.0	10.6	11.3	21.7	7.2	17.0	22.9	11.9	12.6	14.0	22.9	10.1	11.0
<b>pH</b>	7.02	7.36	7.12	7.20	7.65	7.42	7.75	7.56	9.39	8.40	5.72	6.97	7.30	8.11	7.80	7.25
<b>Redox pot. (mV)</b>	+64	+51	+85	+58	+21	+33	+336	+49	-47	+333	+150	+83	+40	+294	+295	+30
<b>EC (µS/cm) Lab.</b>	17.8	72.1	36.2	94.6	58.2	68.2	61.0	100.2	73.8	64.0	30.6	33.8	86.0	167.0	174.0	26.8
<b>Concentration (mg L<sup>-1</sup>)</b>																
<b>Ca</b>	0.85	4.21	2.75	7.20	3.64	5.72	2.10	7.64	7.74	7.51	1.16	1.65	4.06	25.90	16.80	0.62
<b>Mg</b>	0.37	2.97	0.58	4.46	1.19	1.29	4.30	2.53	0.77	0.75	0.72	0.91	1.70	1.79	2.72	0.69
<b>Na</b>	2.45	5.14	3.06	4.99	5.10	4.74	3.68	9.35	4.54	4.36	4.69	3.56	7.62	5.39	8.76	2.20
<b>K</b>	0.18	0.27	0.19	0.53	0.51	0.66	0.27	0.25	0.18	0.23	0.19	0.22	0.33	1.67	1.25	0.20
<b>Sr</b>	bd	bd	bd	bd	bd	bd	bd	bd	bd	bd	bd	bd	bd	bd	bd	bd
<b>NH<sub>4</sub></b>	bd	bd	bd	bd	bd	bd	bd	bd	bd	bd	bd	bd	bd	bd	bd	bd
<b>CO<sub>3</sub></b>	-	-	-	-	-	-	-	-	3.00	0.60	-	-	-	-	-	-
<b>HCO<sub>3</sub></b>	6.10	23.19	10.07	40.27	13.42	18.00	29.72	27.15	20.75	24.41	9.15	9.76	18.31	74.44	57.36	7.93
<b>SO<sub>4</sub></b>	1.29	3.13	1.62	5.35	5.18	7.79	2.08	5.08	3.75	4.16	1.77	2.50	3.51	11.45	8.00	0.92
<b>Cl</b>	2.09	9.18	5.80	5.82	7.35	7.07	4.03	14.25	5.17	4.88	3.95	4.44	12.47	8.20	10.41	2.26
<b>HPO<sub>4</sub></b>	bd	bd	bd	bd	bd	bd	bd	bd	bd	bd	bd	bd	bd	bd	bd	bd
<b>NO<sub>3</sub></b>	bd	bd	bd	bd	0.11	bd	bd	bd	bd	0.22	bd	bd	bd	0.56	0.12	bd
<b>F</b>	bd	bd	bd	bd	bd	0.03	bd	bd	bd	bd	bd	bd	bd	0.08	0.07	bd
<b>Br</b>	bd	0.03	bd	bd	0.03	bd	bd	0.04	bd	bd	bd	bd	bd	0.02	0.02	bd
<b>TDS</b>	13.33	48.12	24.07	68.62	36.53	45.30	46.18	66.29	45.90	47.12	21.63	23.04	48.00	129.50	105.51	14.82

Abbreviations: nd – not determined, bd – below detection limit.

Table 2D. Hydrochemical analyses of water samples collected in ultramafic rocks of the Seiland Igneous Province.

Sample	W7	W8	W9	W12	W13	W18	W20	W21	W23	W26	W19	W16	W17	W22	W10	W11
<b>Geology</b>	Ultram. rock	Ultram. rock, gabbro	Ultram. rock, gabbro													
<b>Minor constit.</b>																
<b>Location</b>	Brook	Lake	Brook, talus	Brook, talus	Spring, talus	Brook	Brook									
<b>Date</b>	22. Jul. 03	22. Jul. 03	22. Jul. 03	23. Jul. 03	23. Jul. 03	26. Jul. 03	26. Jul. 03	26. Jul. 03	28. Jul. 03	31. Jul. 03	26. Jul. 03	25. Jul. 03	25. Jul. 03	25. Jul. 03	22. Jul. 03	22. Jul. 03
<b>Temp. (°C)</b>	9.0	10.0	12.0	12.0	12.0	6.0	12.0	12.0	12.0	11.0	12.0	10.0	13.0	13.0	15.0	14.0
<b>pH</b>	6.68	6.95	7.15	6.65	7.10	7.49	7.26	7.44	7.48	7.06	7.68	7.50	7.57	7.69	7.50	7.70
<b>Redox pot. (mV)</b>	+77	+61	+54	+30	+42	+45	+57	+46	+20	+18	+46	+48	+49	+14	+37	+30
<b>EC (µS/cm) Lab.</b>	17.3	33.6	47.4	37.7	22.0	27.0	41.5	26.0	46.6	25.7	39.9	72.3	76.0	208.0	109.9	107.9
<b>Concentration (mg L<sup>-1</sup>)</b>																
<b>Ca</b>	0.31	0.70	1.31	0.72	0.86	0.54	1.39	0.71	1.00	0.97	1.38	4.72	4.17	7.38	8.14	7.64
<b>Mg</b>	0.45	0.84	1.14	0.86	0.92	1.02	2.02	1.11	1.46	1.76	1.97	2.98	4.02	4.26	3.84	3.34
<b>Na</b>	1.78	3.02	4.68	3.99	1.92	2.98	3.98	2.82	3.62	1.92	3.70	4.71	4.78	6.42	7.28	7.26
<b>K</b>	0.12	0.17	0.30	0.21	0.23	0.18	0.26	0.19	0.25	0.11	0.37	0.43	0.40	0.54	0.90	0.82
<b>Sr</b>	bd	bd	bd													
<b>NH<sub>4</sub></b>	bd	bd	bd													
<b>CO<sub>3</sub></b>	-	-	-	-	-	-	-	-	-	-	-	-	-	-	-	-
<b>HCO<sub>3</sub></b>	6.71	7.32	9.76	5.19	11.59	7.93	21.36	11.59	15.26	10.98	18.92	26.85	26.24	35.39	35.39	32.95
<b>SO<sub>4</sub></b>	0.58	0.98	1.98	1.67	0.56	1.06	1.34	1.06	1.26	2.01	1.33	4.28	4.41	4.79	5.88	5.15
<b>Cl</b>	1.97	3.95	6.65	6.92	1.52	4.41	2.05	2.41	2.89	2.32	2.65	7.41	8.07	9.33	10.64	10.50
<b>HPO<sub>4</sub></b>	bd	bd	bd													
<b>NO<sub>3</sub></b>	bd	bd	0.09													
<b>F</b>	bd	bd	bd													
<b>Br</b>	bd	bd	0.04													
<b>TDS</b>	11.92	16.98	25.82	19.56	17.60	18.12	32.40	19.89	25.74	20.07	30.32	51.38	52.09	68.11	72.10	67.79

Abbreviations: nd – not determined, bd – below detection limit.

Table 2E. (continuation). Hydrochemical analyses of water samples collected in the gabbro-dominated terrain of the Seiland Intrusive Complex.

Sample	W60	W61	W62	W63	W69	W70	W82	W74	W78	W30	W53	W68	W79	W83	W84
<b>Geology</b>	Granite	Granite	Granite	Granite	Gneiss	Gneiss	Gneiss	Gneiss, granite	Gneiss, granite	Gneiss, marmor	Sandstone	Calc-pelitic-schist	Meta-basalte, calcite	Gabbro, gneiss, sandstone	Sandstone, gneiss, gabbro
<b>Minor constit.</b>															
<b>Location</b>	Brook	Brook	Brook	Tunnel, drops	Brook	Brook	Brook	Lake	Dripping water	Brook	Brook	Brook	River	River	River
<b>Date</b>	17. Aug. 03	17. Aug. 03	17. Aug. 03	17. Aug. 03	11. Aug. 09	11. Aug. 09	16. Aug. 09	14. Aug. 09	15. Aug. 09	02. Aug. 03	12. Aug. 03	11. Aug. 09	16. Aug. 09	17. Aug. 09	17. Aug. 09
<b>Temp. (°C)</b>	18.9	18.7	18.2	19.3	11.7	11.8	7.3	22.9	22.3	10.2	12.3	10.1	15.7	15.6	15.6
<b>pH</b>	5.84	6.10	5.93	5.88	7.75	7.55	6.12	7.13	7.73	7.95	8.13	7.65	7.77	7.06	6.71
<b>Redox pot. (mV)</b>	+143	+139	+150	+100	+352	+379	+398	+348	+378	+20	+9	+396	+340	+403	+339
<b>EC (µS/cm) Lab.</b>	12.8	10.9	21.9	40.7	24.0	31.0	24.0	59.5	129.0	112.4	155.8	48.4	53.0	26.0	37.0
<b>Concentration (mg L<sup>-1</sup>)</b>															
<b>Ca</b>	0.39	0.31	0.55	6.47	1.68	2.64	0.95	4.80	15.20	10.43	12.45	5.02	5.25	1.85	3.52
<b>Mg</b>	0.19	0.14	0.35	0.16	0.39	0.49	0.41	0.80	1.67	5.22	6.87	1.22	1.02	0.45	0.90
<b>Na</b>	1.76	1.36	2.65	2.10	1.70	1.91	1.96	4.96	7.17	5.45	13.10	1.90	2.27	1.27	1.42
<b>K</b>	0.20	0.13	0.16	0.59	0.29	0.51	0.18	0.58	1.86	0.53	0.80	0.57	0.38	0.50	0.63
<b>Sr</b>	b.d.	b.d.	b.d.	b.d.	b.d.	b.d.	b.d.	b.d.	b.d.	b.d.	b.d.	b.d.	b.d.	b.d.	b.d.
<b>NH<sub>4</sub></b>	b.d.	b.d.	b.d.	b.d.	b.d.	b.d.	b.d.	b.d.	b.d.	b.d.	b.d.	b.d.	b.d.	b.d.	b.d.
<b>Alk (CO<sub>3</sub>)</b>	-	-	-	-	-	-	-	-	-	-	-	-	-	-	-
<b>Alk (HCO<sub>3</sub>)</b>	2.75	2.44	3.66	11.17	2.14	7.44	1.71	17.94	53.39	51.26	67.73	17.09	23.49	7.63	17.70
<b>SO<sub>4</sub></b>	0.98	0.92	1.03	3.74	4.48	3.91	3.50	1.66	6.93	2.46	4.24	3.97	2.10	2.51	1.67
<b>Cl</b>	1.97	1.52	4.92	2.22	2.41	2.37	3.36	8.88	8.67	7.59	15.69	2.75	3.37	1.41	1.65
<b>HPO<sub>4</sub></b>	b.d.	b.d.	b.d.	b.d.	b.d.	b.d.	b.d.	b.d.	b.d.	b.d.	b.d.	b.d.	b.d.	b.d.	b.d.
<b>NO<sub>3</sub></b>	0.11		0.08	0.35	0.07	0.06	0.17	b.d.	0.06	b.d.	b.d.	0.22	0.07	0.01	0.07
<b>F</b>	0.05	0.09	0.11	2.15	b.d.	b.d.	b.d.	b.d.	b.d.	b.d.	b.d.	b.d.	b.d.	b.d.	0.02
<b>Br</b>	b.d.	b.d.	b.d.	b.d.	b.d.	b.d.	b.d.	b.d.	b.d.	b.d.	0.06	b.d.	b.d.	b.d.	b.d.
<b>TDS</b>	8.40	6.91	13.51	28.95	13.16	19.33	12.24	39.62	94.95	82.94	120.94	32.74	37.95	15.63	27.58

Samples not shown in Fig. 2: W60–W63: Stetind, W53: Island Skorpa, W79: Storelva, W83: Navitelva, W84: Kvaenagselva.

Abbreviations: nd – not determined, bd – below detection limit.



Figure 3. Fieldwork on Seiland.

The locations of the water samples collected in granite- or gneiss-dominated terrains are given in Table 2E. The samples collected in the granite-dominated terrain originate from the immediate vicinity of the Stetind ( $68^{\circ}09'54''\text{N}$ ,  $16^{\circ}35'33''\text{E}$ , elevation: 1392 m) and the Stetind tunnel (about sea level). Samples taken in gneiss-dominated terrains were collected in rivers (Table 2E) just south of the area presented in the geological map (Fig. 2).

### Sampling methodology

Water samples for chemical analyses were collected in 500 ml acid-cleaned polyethylene bottles (Fig. 3). From each location a duplicate was taken. Care was taken to fill the bottles completely to avoid gas exchange. Temperature, pH-value, Redox potential and electrical conductivity (EC) were measured in the field. Immediately after sampling, alkalinity was determined by titration with 0.1 N HCl to a certain pH end point by using a pH-meter, whereas waters with  $\text{pH} > 8.3$  had to be titrated to  $\text{pH} = 8.3$  and  $\text{pH} = 4.3$ . According to the very low mineralisation (low EC) of all water samples,

precipitation was not expected. Nevertheless, all water samples were stored in a refrigerator until they were analysed in the laboratory.

Rain- and sea-water (Table 2A; Fig. 2) were collected as reference samples for the field study and to have the opportunity to consider possible influences concerning the input via precipitation and/or sea spray, when studying silicate weathering processes. Rainfall was collected during single storm events using a polyethylene bottle with a huge polyethylene funnel. Sea-water sampling was carried out by boat at about 1 m depth below the sea surface also using polyethylene bottles.

The water samples from boreholes in the mine were collected after a longer flow period, to avoid contamination with water stored in the borehole. However, all boreholes showed 'artesian' behaviour, i.e., free outflow. Fracture seepage samples from the mine and the two tunnels were collected directly at the 'outflow' points. Surface water samples from brooks, rivers or springs in talus were collected directly in the flowing water. The thickness of the accumulation of broken rock debris (talus) was low.

Alteration materials such as 'white crusts' on rock surfaces were collected by using a knife and storing the samples in small plastic bags.

Care was taken to sample unaltered rock material by using a heavy hammer and a chisel to avoid weathering crusts or fractures in the collected rocks.

## Analytical methods

Optical polarisation microscopy and X-ray fluorescence analyses were performed on the rock samples. The 'white crust' has been exclusively investigated by X-ray diffraction analysis. The composition of minerals in the rock samples was determined by electron probe microanalysis (EPMA) using the CAMECA SX100 instrument at the IMPG (Institute of Mineralogy Petrology and Geochemistry, University of Freiburg). EPMA is a tool to determine non-destructively the chemical composition of small volumes of solid materials. All quantitative analyses were made using the wavelength dispersive spectrometers of the instrument. The acceleration voltage was 15 kV, the beam-current 10 nA and the counting times 10 s. Analyses were made using a focused electron beam (2  $\mu\text{m}$  spot size) except for Na and K measurements in mica and alkali-feldspar where a defocused beam was used (c. 10  $\mu\text{m}$ ). The instrument was calibrated for each element analysed using well characterised natural materials as standards. Data reduction was performed by utilising software provided by the manufacturers of the instrument. The results of the whole-rock chemistry, major and trace elements, are presented in Table 1.

The chemical composition of the water samples was determined in the laboratory of the IMPG after filtration through cellulose acetate membrane filters with a 0.45  $\mu\text{m}$  pore size, using ion chromatography for the anions (Dionex 120) and atomic absorption spectroscopy for cations (AJ Vario 6). Detection limits for Ca, Sr, F, Br and  $\text{NO}_3^-$  are 50  $\mu\text{g L}^{-1}$ , for Na, K, Li and Mg 20  $\mu\text{g L}^{-1}$ , for Cl 500  $\mu\text{g L}^{-1}$ , for  $\text{PO}_4^{3-}$  100  $\mu\text{g L}^{-1}$  and for  $\text{SO}_4^{2-}$  800  $\mu\text{g L}^{-1}$ . Si was not analysed. The total of dissolved solids (TDS) has been calculated from the analyzed concentrations. The analytical data of the water samples are presented in Table 2A–E.

The overall charge error of the analyses expressed as electroneutrality (EN) was calculated from ( $\text{meq L}^{-1}$ ):

$$\text{EN} = 100 * (\text{sum of cations} - \text{sum of anions}) / (\text{sum of cations} + \text{sum of anions}) \quad (4)$$

The average EN for all 100 samples was <4%. In 6 samples the EN was >10%. High EN values were predominantly calculated for very low TDS waters, because small analytical errors may lead to high EN values. With the exception of just two samples, all collected and analysed samples were used for this paper.

## Results of investigated rock samples

In this chapter, a selection of the rock samples collected during fieldwork is described, comprising rocks typical of the Seiland Igneous Province including carbonatite, nepheline-syenite, gabbro and ultramafic rocks. Fig. 2 shows the locations of these rock samples. Most of the mineralogical and geochemical investigations were carried out within the context of two master theses (Teiber, 2010; Jendryszczyk, 2013) and one PhD thesis (Li, 2013) at the University of Freiburg under the supervision of the first and fifth author. Based on the medium- and coarse-grained appearance of all samples the rocks can generally be classified as plutonic.

The mineralogy and petrochemistry of **carbonatites** were previously investigated by Strand (1951, 1981) and Bruland (1980). According to Woolley & Kempe (1989) they could be characterised as calcium-rich silicocarbonatites. The collected carbonatite samples (Fig. 2) are medium- to coarse-grained plutonic rocks consisting of varying amounts of calcite, amphibole, biotite, apatite and Fe-Ti oxides, whereas calcite is the only carbonate phase. Table 1 shows the results of the XRF analyses of the whole-rock chemistry, where according to custom the major elements are expressed as oxides in wt.% and the trace elements in ppm. An average whole-rock composition of 26 wt.%  $\text{SiO}_2$  and 18.3 wt.% CaO has been measured. The MgO content varies from 2.1 to 3.8 wt.% and  $\text{P}_2\text{O}_5$  between 0.8 wt.% and 1.4 wt.%, whereas phosphorus is incorporated in apatite (Jendryszczyk, 2013). The carbonatite samples are quite rich in alkalis (>4.8 wt.%) and contain high amounts of  $\text{Al}_2\text{O}_3$  (8.44–14.69 wt.%), corresponding to the large proportion of observed aluminosilicate minerals. Furthermore, in the silicocarbonatites a high enrichment of trace elements such as barium (Ba) and strontium (Sr) is detected (Jendryszczyk, 2013). These results are in line with the investigations of NGU (Geological Survey of Norway) presenting mean values based on 65 samples (Gautneb, 2009; Heim et al., 2010). They found that the silicocarbonatites contain about 30% biotite, 40% calcite and 7.5% apatite and detected unusually high Ba- and Sr-concentrations in the carbonatites, with barium mainly in biotite and strontium mainly in calcite.

Two different calcite phases were observed by Jendryszczyk (2013): a primary crystallised SrO–FeO-rich and MnO-poor phase with about 2 wt.% SrO and a secondary SrO–FeO-poor and MnO-enriched phase, partly replacing the primary one. In addition, MgO is about 10 times higher in the primary phase (~0.35 wt.%) than in the secondary phase. Biotites are Ba-rich with 0.24–3.77 wt.% BaO and contain about 28 wt.% FeO and 8 wt.%  $\text{K}_2\text{O}$ . Apatites and two types of amphibole are also major mineral phases in the silicocarbonatites. Other accessory minerals like feldspar, nepheline, pyrite and zircon show an irregular distribution and are not present in all samples (Jendryszczyk, 2013).

On a macroscopic scale, Bruland (1980) observed intrusive carbonatite veins within the nepheline-syenite. However, the collected **nepheline-syenite** samples show some few, small, white reaction veins with bilateral, slightly reddish, reaction zones, whereas the fresh nepheline-syenite has a greyish colour. Table 1 lists three XRF analyses of the nepheline-syenite samples, where samples 1145 and 1147 are from the underground mining area inside the tunnel and sample 1151 from the open pit on top of mount Nabbaren. Compared with the carbonatite rocks, the nepheline-syenites contain lower concentrations of  $\text{Fe}_2\text{O}_{3(\text{tot})}$ , MgO, CaO and almost no  $\text{P}_2\text{O}_5$ , whereas the contents of  $\text{Na}_2\text{O}$  and  $\text{K}_2\text{O}$  are strikingly increased. In addition, a slight enrichment of Sr and Ba can be observed, but with lower concentrations than in the carbonatites (Li, 2013). The analytical data are in good agreement with the data (mean value and variance of 65 analyses) published in Gautneb (2009).

The collected nepheline-syenite is mainly composed of K-feldspar (40%), nepheline (35%), amphibole (10%) and clinopyroxene (5%), with accessory biotite, apatite, titanite, magnetite, ilmenite, calcite and zeolite. There is no significant difference in mineral constituents between the original slightly grey rock matrix and the more reddish, stronger altered, reaction zones, whereas the white reaction veins are composed of fine-grained zeolite aggregates (thomsonite and natrolite overgrown with thomsonite) (Li, 2013).

The composition of the mineral nepheline can generally be expressed as a solid solution between the three end-members: ideal sodic nepheline ( $\text{Ne} - \text{NaAlSiO}_3$ ), kalsilite ( $\text{Ks} - \text{KAlSiO}_4$ ) and quartz ( $\text{Qtz} - \text{SiO}_2$ ). The mineral chemistry of the investigated nepheline showed variations in composition between  $\text{Ne}_{80}\text{Ks}_{20}\text{Qtz}_1$  and  $\text{Ne}_{77}\text{Ks}_{18}\text{Qtz}_4$  without systematic differences. An average Na/K ratio in the nepheline of 3.95 was detected with a variance of 3.63–4.33. The investigated K-feldspars showed a Na- and K-rich lamella texture and thus two main composition groups without an An component:  $\text{Ab}_{15-30}$  and  $\text{Or}_{65-86}$  (An – anorthite, Ab – albite, Or – orthoclase). Additionally, Li (2013) detected some ternary-phase feldspars with a variable composition and a low An component. According to the international nomenclature (Leake et al., 2004), the amphiboles are Ca- and Al-rich hastingsites and ferro-paragasites.

Table 1 lists the results of the XRF analyses of the **gabbro and ultramafic rock** samples, and Fig. 2 shows the localities where the samples were collected. By means of CIPW Norm calculation, originally developed by the petrologists Cross, Iddings, Pirsson and the geochemist Washington to determine a set of idealised mineral-like components from a bulk chemical analysis of a rock, the chemical analyses were recalculated – using the excel spreadsheet written by Hollocher (2007) – and the samples accordingly characterised. Thus, samples 1246, 1027, 1046, 1028, 1054, 1224, 1281, 1115 and 1245

are gabbros and samples 1110 and 1113 are ultramafic rocks, because they contain no or almost no plagioclase (Plg). The gabbro samples 1246, 1046, 1028, 1054, 1281, 1115 and 1245 could be characterised as olivine-gabbros, because they contain the minerals plagioclase (Plg), pyroxene (Px) and olivine (Ol). Gabbro sample 1027 could be classified as anorthosite because of its very high Plg-content and sample 1224 as troctolite, showing a very low Px content. In the gabbros, all calculated plagioclases show very high An/(An + Ab) ratios (55–79 vol.%). In contrast to the gabbros, the ultramafic rock samples 1110 and 1113 are composed mainly of olivine (Ol) and pyroxene (Px) and thus could be characterised as peridotites, showing very high MgO contents in the XRF analyses (Table 1). The results of the CIPW Norm calculation are in good agreement with the findings of the polarisation microscopy.

The higher MgO contents in some samples (Table 1) seem to be caused mainly by small amounts of olivine. The CaO contents can be assumed to be related, on the one hand, to the amount of clinopyroxenes and amphiboles detected by means of the polarisation microscopy and, on the other hand, to the amount of plagioclase present in the gabbro samples. The peridotite samples 1110 and 1113 are characterised by very low alkali and silica contents (<0.3 and <40 wt.%, respectively) in contrast to the gabbro samples (0.7–3.7 wt.% and 41–51 wt.%; Table 1). Ni shows higher concentrations in the peridotites (c. 1100 ppm), respectively in the olivine-bearing gabbros where Ni is supposed to be mainly incorporated in olivine. Cr is also found with higher concentrations in the two peridotites (c. 2000 ppm), presumably incorporated in the spinels or in other minerals like pyroxene. The Sr contents are higher in the classified gabbro samples (200–1000 ppm) relative to the ultramafic samples (<50 ppm). For example, Sr may probably substitute for Ca in the plagioclases. In addition, Ba contents are generally also higher in the gabbros than in the ultramafic rock samples.

Electron probe microanalysis (EPMA) of 36 **plagioclases** in the rock samples 1028, 1281 and 1046, characterised as olivine-gabbro, and in the troctolite sample 1224 has shown noticeable variations in chemical composition from sample to sample, but the geochemical range of the major elements is quite low (Teiber, 2010). All plagioclases in the olivine-gabbros (Table 1) show a significantly higher anorthite ( $\leq 80$  mol.%) than albite component, whereas the plagioclase in the troctolite sample 1224 has significantly lower An and Ab contents. However, all plagioclases are Ca-rich, and are in line with the CIPW Norm analyses.

Analogous investigations were carried out on 21 **pyroxenes** in the above-mentioned olivine-gabbros (1028, 1281), in the troctolite (1224), and in the peridotite sample 1113. Taking into account the high Ca and Mg content, the pyroxenes could be classified

as clinopyroxenes ((Mg, Fe) Ca Si<sub>2</sub>O<sub>6</sub>). Expressing the cation-proportions as wollastonite (Ca<sub>2</sub>Si<sub>2</sub>O<sub>6</sub>), enstatite (Mg<sub>2</sub>Si<sub>2</sub>O<sub>6</sub>) and ferrosilicate (Fe<sub>2</sub>Si<sub>2</sub>O<sub>6</sub>), the average enstatite (En) is about 39–46 mol.% and wollastonite (Wo) about 46–49 mol.%. The lower En- and Wo-mol.% corresponds to the troctolite sample 1224, showing higher Fe contents (ferrosilicate: c. 15 mol.%). EPMA analyses of *amphibole* in the olivine-gabbro samples 1046 and 1281 and in the troctolite sample 1224 showed that amphiboles could be classified as calcic amphiboles, characterised by high Al<sub>2</sub>O<sub>3</sub> and high TiO<sub>2</sub> contents in comparison with pyroxenes. The majority of the analysed *olivines* in the olivine-gabbros 1028 and 1281 and in the peridotite sample 1113 are Mg-rich, whilst the troctolite sample 1224 comprises Fe-richer olivines. In general, all olivines exhibit a relative high amount of NiO (Teiber, 2010).

The XRD pattern of the weathering surface (white crust) on the olivine-gabbro sample 1046 suggests that the crust consists of Ca- and Na-bearing zeolites (Teiber, 2010). According to Bucher & Stober (2000), the formation of this mineral most probably originates from the rock sample itself, due to weathering of Ca-rich plagioclase.

## Results of the water analyses

Standard sea-water is highly mineralised (TDS about 38 g/kg) in the open temperate and tropical oceans as a consequence of little rainfall and high evaporation (Table 2A), whereas in cold seas with melting ice the mineral concentration is significantly lower (TDS about 30 g/kg). Generally, sea water has a slightly alkaline pH in the range 7.5 to 8.4. Two *seawater* samples (WS6, WS54) were collected in 2003 and 2009 at different locations (Fig. 2; Table 2A). The pH values of the samples are in the order of 8.2 and the TDS about 30 g/kg, typical for ocean waters at latitude >70°N. The dominant ions in the collected sea-water samples are Na and Cl with elevated Mg concentrations, which are characteristic values for sea-water (Nordstrom et al., 1979). Surprisingly, both samples have different TDS, 29.7 g/kg and 31.1 g/kg, respectively. Sample WS6, collected within the Kvænangen fjord, has a significantly lower concentration than sample WS54, sampled in the ocean at a greater distance from the fjords (Fig. 2). The difference might be an effect of inflow of water from rivers and brooks and/or of density layering in the more sheltered fjord compared to the open ocean, where water circulation and mixing is more intensive. Nevertheless, both sea-water samples (WS6, WS54) show Na/Cl ratios in the same order, 0.80 and 0.81, respectively.

The *rainwater* sample (Table 2A) collected in 2009 (WR76) would seem to be more meaningful than the one from 2003 (WR59), since the intensity of the rainfall was much higher and accordingly it was possible to collect

a greater amount of water and fill the bottle completely. Nevertheless, the two analytical results differ only slightly from each other. Both samples show a very low TDS of about 7 mg L<sup>-1</sup>. Rainfall is acidic with pH = 4.64. The low pH is mainly caused by natural dissolved CO<sub>2</sub> yielding an acidic pH of around 5.0. The presence of small amounts of sulphuric and nitric acid in rainwater is most probably the reason for the observed slight reduction of pH (see below). If calcite is present in the bedrock, it buffers the pH of the acidic rainwater input very rapidly; otherwise rainwater produces low pH waters in the catchments. The dominating ions in rainwater are Na and Cl with a molar-ratio of Na/Cl = 0.80 in the 2009 sample, and thus showing that the hydrochemistry of rainwater is strongly influenced by seawater. Rainwater also contains small amounts of calcium, magnesium and potassium. Hydrogen, carbonate, sulphate and nitrate could be detected too. While the Mg/Na ratio in rainwater is in the same order of magnitude as in seawater, the SO<sub>4</sub>/Cl ratio is slightly higher.

Most *surface water* samples were collected in small brooks along the coastline, but some samples were taken in small lakes and brooks farther inland on the islands or the peninsula. Three samples were collected from within road-tunnels and 10 samples within the nepheline-syenite mine at Lillebukt in the south of Sternøya (Fig. 2; Table 2B–E). Since the investigated area is very sparsely inhabited, the water samples in this study are not affected by anthropogenic activity with the exception of a few samples from the nepheline-syenite mine.

The temperature of the collected water samples is low, generally about 6°–22°C (Table 2B–E). The pH value varies between acidic with pH = 5.45 (W65) and alkaline with pH = 9.39 (W5). All water samples are negligibly mineralised with TDS between 7 mg L<sup>-1</sup> (W66) and 118 mg L<sup>-1</sup> (W75). The highest TDS values, >80 mg L<sup>-1</sup>, have been detected in waters circulating in carbonatite rocks and in waters of the nepheline-syenite underground mine. TDS values >50 mg L<sup>-1</sup> are found in springs from talus material of gabbro and ultramafic rocks and in brooks passing across a carbonatite-dominated terrain or in waters collected in the nepheline-syenite underground mine. The lowest TDS values, <20 mg L<sup>-1</sup>, originate from brooks in granitic or metamorphic rocks or sandstones, from small brooks in compact gabbro or ultramafic rock complexes and from glacier lakes.

Dissolved silicon (Si) was not analysed, such that in the discussion section various assumptions have had to be made regarding the likely saturation status of the waters with respect to silica minerals. However, there is no evidence that surface water or groundwater are saturated with respect to chalcedony or quartz, since silica sinter was never observed during sampling.

In the following, the water samples are grouped in different so-called Schoeller-diagrams (Fig. 4A–F) with

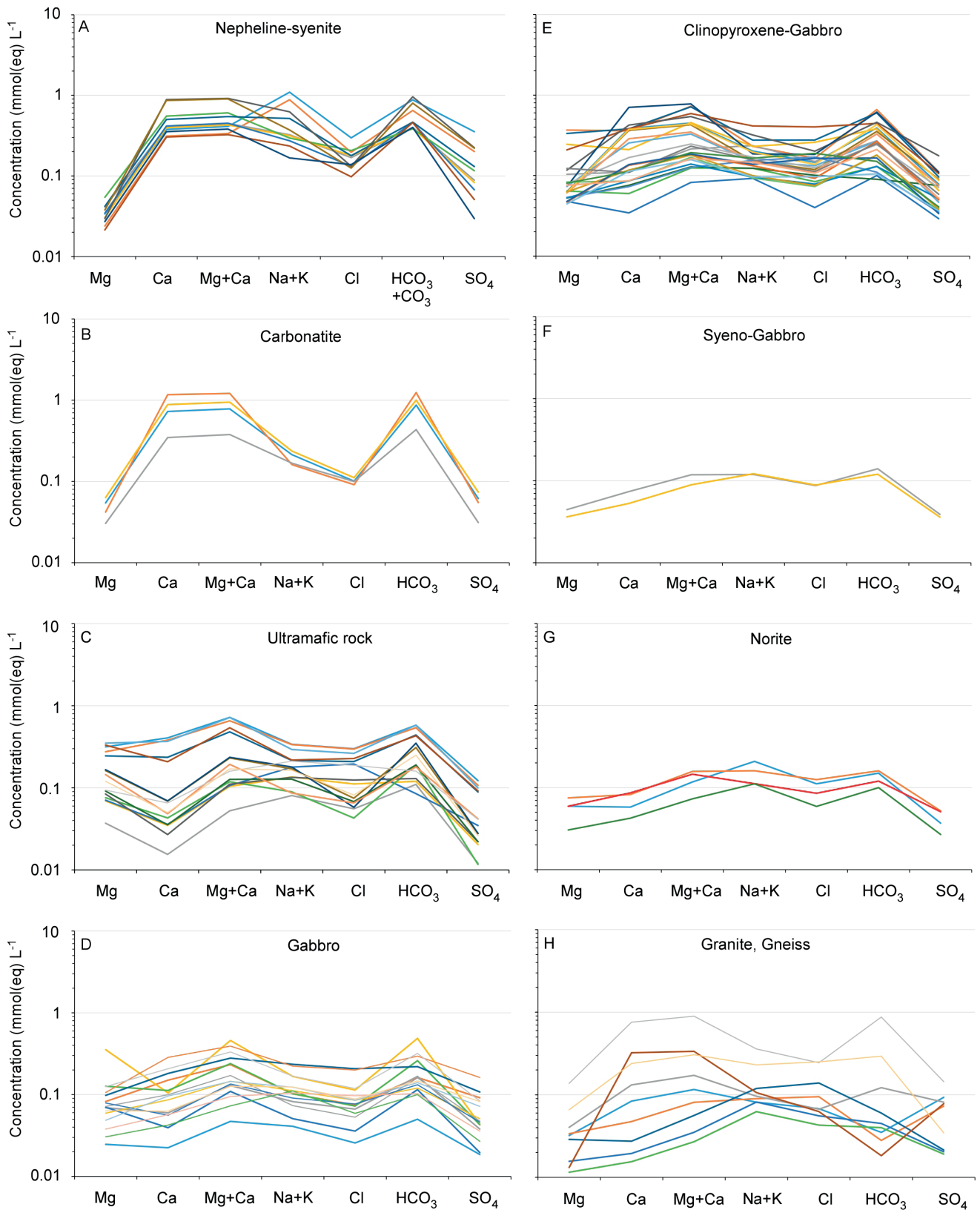


Figure 4. (A–H) Schoeller-diagrams of waters collected in geologically different catchments. (A) see Table 2B (samples W31–41), (B) see Table 2B (samples W42–45), (C) see Table 2D (samples W7–13, 16–23, 26), (D) see Table 2C (samples W27, 28, 55, 56, 64–67, 71, 89–91, 93, 96, 97, 100), (E) see Table 2C (samples W1, 2, 5, 14, 15, 29, 46–52, 72, 73, 80, 81, 85–88, 92, 94, 95, 98, 99), (F) see Table 2C (samples W3, 4), (G) see Table 2C (samples W27, 28, 57, 58), (H) see Table 2E (samples W60–63, 69, 70, 74, 78, 82).

respect to the geology of the catchment area, where they were collected. It is important to mention that the collected samples may not exclusively be affected by the geology of the catchment as shown in the map, since in some cases there are additional small outcrops with a different lithology which cannot be shown in the scale of the map (Fig. 2). Thus, some water samples are hydrochemically affected by these 'small outcrops'. In addition, within the nepheline-syenite mine relatively high nitrate concentrations of up to 17 mg L<sup>-1</sup> were measured deriving probably from the explosives used in mining.

As mentioned earlier, the Lillebukt Alkaline Complex (Fig. 2) consists mainly of carbonatites, nepheline syenites, metagabbros and hornblendites. The chemical properties of the water samples within the **nepheline-syenite mine** inside the mountain Nabbaren clearly show a dependency on the thickness of the overburden. Thus, TDS is increasing with depth. The TDS near the top of the mountain (c. 700 m a.s.l.) is about 41 mg L<sup>-1</sup>, whereas deep inside the mountain (c. 100 m a.s.l.) the TDS is 118 mg L<sup>-1</sup>. This overall increase, with respect to the cations, is mainly caused by an increase in sodium but also by calcium and potassium, while magnesium shows no depth dependency (Fig. 4A; Table 2B). The water samples of the nepheline-syenite mine have the highest pH values of all samples. Water samples in the mine are alkaline with pH values generally between 8.05 and 9.36, with the exception of one dripping water sample from the tunnel ceiling (pH = 7.48).

Surface waters sampled within the **carbonatite rocks** of the island Sternøya (Fig. 2; Table 2B) have TDS of about 100 mg L<sup>-1</sup> and are thus the samples with the highest TDS observed in surface waters. Waters are mainly composed of calcium and hydrogen carbonate, whilst magnesium and sulphate contents are low (Fig. 4B). PH of these waters fluctuates between 7.72 and 8.05, reflecting a calcite buffering system. In the carbonatite rocks pH is significantly lower than in the waters of the nepheline-syenite mine.

On the island Seiland, many samples were collected from small brooks and lakes situated in **ultramafic rocks** (Fig. 2; Table 2D). Waters sampled in ultramafic rocks typically have elevated magnesium concentrations (Fig. 4C). The pH of the ultramafic water samples is circumneutral (6.65–7.69), whereas waters sampled in the ultramafic talus material (W16, W17, W22) have pH values in the upper range of the interval. TDS values of the water samples are between 11.9 and 68.1 mg L<sup>-1</sup> and thus generally lower than the waters collected in the nepheline-syenite mine or in carbonatite rocks. The 3 water samples from ultramafic talus material show TDS of more than twice (51.4–68.1 mg L<sup>-1</sup>) the values of samples from compact ultramafic material (11.9–32.4 mg L<sup>-1</sup>), probably caused by the enhanced contact surface area and residence time in the talus material. The much

higher TDS are especially caused by higher calcium, sodium and magnesium concentrations. Nevertheless, potassium is slightly increasing too with TDS. The waters collected in ultramafic rocks belong to a Na–Mg (Ca)–HCO<sub>3</sub><sup>-</sup> or Na–Mg–HCO<sub>3</sub><sup>-</sup> type, when residence time is short (water samples from compact rocks), and they seem to develop to a Mg–Ca–Na–HCO<sub>3</sub><sup>-</sup> type with a more prolonged residence time and enhanced contact surface area (ultramafic talus material; Fig. 4C).

The TDS in water samples collected in 'ordinary' **gabbro**-dominated terrain (Fig. 2; Table 2C) is generally low, in most cases even <30 mg L<sup>-1</sup>. In gabbroic talus material waters show a significantly higher TDS, up to 45 mg L<sup>-1</sup>. Elevated TDS values (46 mg L<sup>-1</sup>, 48 mg L<sup>-1</sup>) were also recorded in the two samples collected in the Øksfjordtunnel (W5, W99). The pH of the gabbro samples is circumneutral, with the exception of the two samples collected in the Øksfjordtunnel which show alkaline values. Water type in gabbro rocks is quite variable, thus Na-, Mg- and Ca-dominated waters are found, all with HCO<sub>3</sub><sup>-</sup> as a main anion component (Fig. 4D). Since TDS is generally low, Cl is sometimes also one of the main anions. Waters collected in **clinopyroxene-gabbro**, foliated **syeno-gabbro** or **olivine-gabbro** rocks (Fig. 2) strongly resemble waters in 'ordinary' gabbro material (Fig. 4E, F), with the exception that the TDS of waters in clinopyroxene-gabbro generally might be slightly higher. The two water samples collected in syeno-gabbro have very low TDS (Fig. 4F). Whereas waters collected in clinopyroxene-gabbro mostly have higher Ca concentrations than waters circulating in 'ordinary' gabbro (Fig. 4E, D), the low-concentrated samples from the syeno-gabbro have relatively high Na concentrations. Water samples collected in **norite** resemble those in syeno-gabbro, but show a slightly elevated TDS (Fig. 4G).

Since conditions are oxidizing in surface water or shallow groundwater, Fe and Al (not analysed) are generally low as pH is circumneutral in waters collected in gabbro- and ultramafic rock catchments. However, filtration of water samples in the laboratory might remove any precipitates or colloids if present, leading to an underestimation of dissolved Fe contents in the waters.

Water samples collected in **granite** and **gneiss** catchments reveal rather diverse Schoeller-patterns (Fig. 4H; Table 2E). The majority of the samples were collected in gneisses, which have higher TDS and are dominated by Ca and HCO<sub>3</sub><sup>-</sup> (W69, W70, W74, W78), whereas waters collected in granites are lower concentrated and seem to be dominated by Na and Cl (W60–W62).

The Piper-diagram (Fig. 5) shows the distribution of the main components of all collected water samples. According to Fig. 5 the waters are subdivided in certain subgroups dependent on the lithological properties of the rocks, in which the waters are circulating. Thus, waters in carbonatite- and nepheline-syenite-dominated

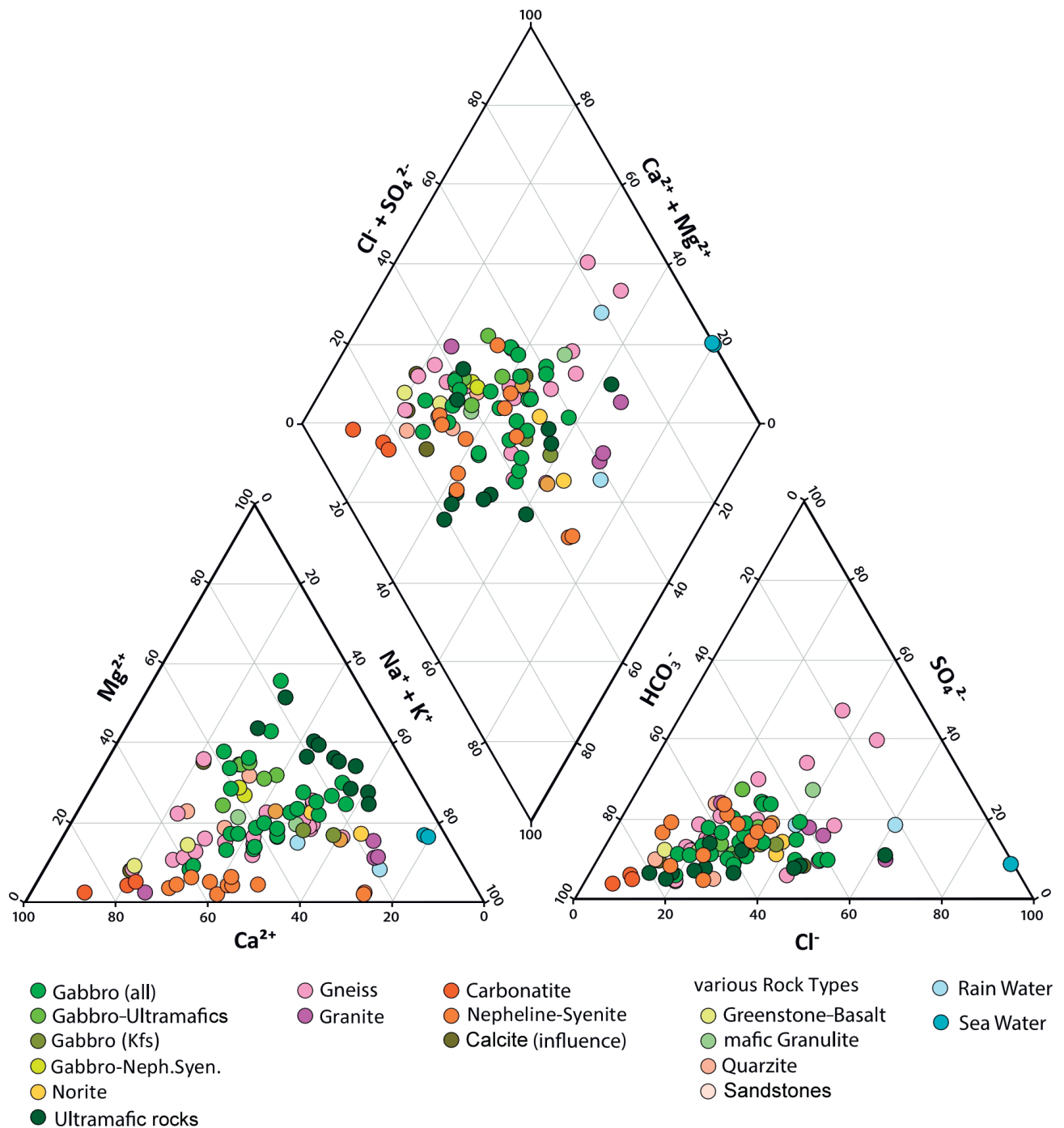


Figure 5. Piper-diagram of all collected water samples showing various subgroups. Anions and cations presented in eq. %.

terrains contain very low Mg- and high Ca-portions, whilst waters circulating in gabbros or ultramafic rocks show proportionally much higher Mg and lower Ca. Waters in granites and gneisses are somewhere in between. In contrast to the Piper-diagram (Fig. 5) the Schoeller-diagrams (Fig. 4A–H) show additionally the waters' mineralisation, while a Piper-diagram has the advantage that many more analyses could be plotted in the figure.

## Discussion

Generally, TDS are, amongst other things, a function of residence time, reactive surface area, degree of alteration and the mineralogical composition of the rock. Prolonged residence time and enhanced water-rock interaction as a result of a larger reactive surface area and increased degree of alteration of talus material are expected for waters circulating in a comparable terrain. Thus, enhanced TDS are observed there.

The distribution of species and saturation states of the waters were calculated using the geochemical code Phreeqc (Parkhurst & Appelo, 1999). The saturation index (SI) relates the ion activity product (IAP) to the equilibrium constant (K) of the dissolution reaction of a considered mineral at a given P and T:  $SI = \log(IAP/K)$ . However, using the code Phreeqc and the llnl database (Parkhurst & Appelo, 1999), all collected water samples (with exception of the two sea-water samples) are undersaturated ( $SI < 0$ ) with respect to all possible solids, dependent on the analysed, respectively analytically detectable parameters in the water samples (Table 2B–E). Taking the whole hydrogeological situation of the relatively short circulation time into account, most water samples could be undersaturated with respect to quartz.

According to Bruland (1980) and Gautneb (2009), carbonatite vein intrusions and/or calcite-rich mafic dykes are occurring in nepheline-syenites. In gneisses, fractures filled with precipitates of calcite or Ca-zeolites are quite common (Bucher & Stober, 2000). Thus, some water samples in these lithological units show a possible additional source of Ca, probably from locally occurring Ca-carbonate minerals (e.g., calcite:  $CaCO_3$ ).

### Marine influence

All surface water samples showed significant amounts of chloride between  $0.91 \text{ mg L}^{-1}$  and up to  $15.69 \text{ mg L}^{-1}$ , even though the minerals of the rocks of the Seiland Igneous Province have no chloride bound in their mineral lattice.

The Cl/Br ratio (mg-basis) of the two sea-water samples (WS6, WS54) is 273 and 281, respectively, corresponding to Cl/Br investigations of recent seawater worldwide (e.g., Braitsch & Herrmann, 1963; Stober & Bucher, 1999a; Rao et al., 2005). Since the TDS of most water samples collected in the Seiland Igneous Province are quite low, bromide could be detected in only a few samples (15 Br data) with values of  $Br \leq 0.06 \text{ mg L}^{-1}$ . Most of these samples showed the measured sea-water signature in Cl/Br. Two samples had slightly higher Cl/Br values, but bromide analysed in these samples was very low ( $Br = 0.02 \text{ mg L}^{-1}$ ), actually below the detection limit. Thus, the chloride in the water samples with reliably detectable bromide concentrations had a sea-water signature, i.e., the origin of chloride is most probably marine.

To obtain some further information concerning the marine influence on the collected water samples, a closer look was taken at the Na/Cl ratio (mol-basis), which is  $Na/Cl = 0.8$  for seawater (Fig. 6). The rainwater sample WR76 has the same Na/Cl ratio as seawater. As mentioned before, rainwater sample WR59 is of lower

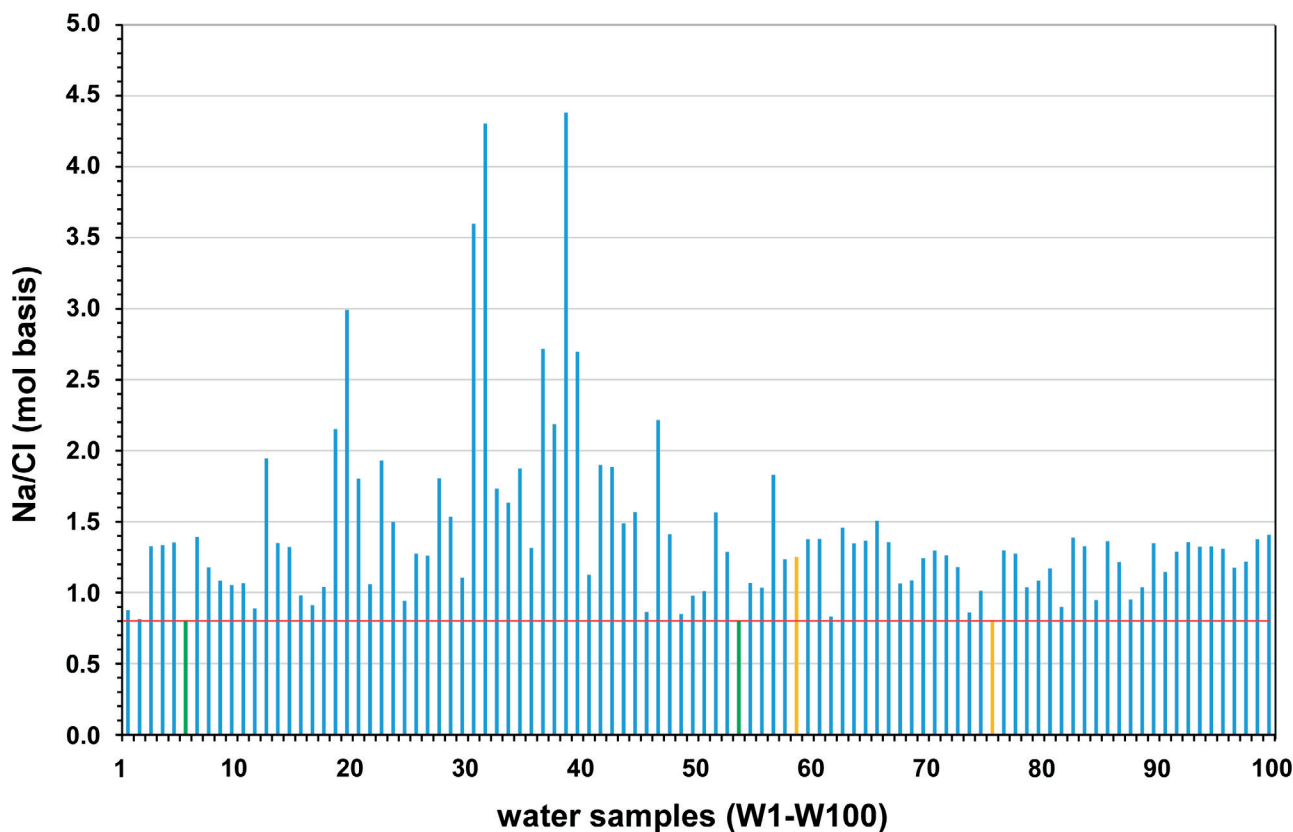


Figure 6. Na/Cl (mol-basis) of all water samples. Sea-water samples (WS6, WS54) are in green and rainwater samples (WR59, WR76) in yellow (please note: rainwater sample WR59 is of minor quality). There are no samples with  $Na/Cl < 0.8$ .

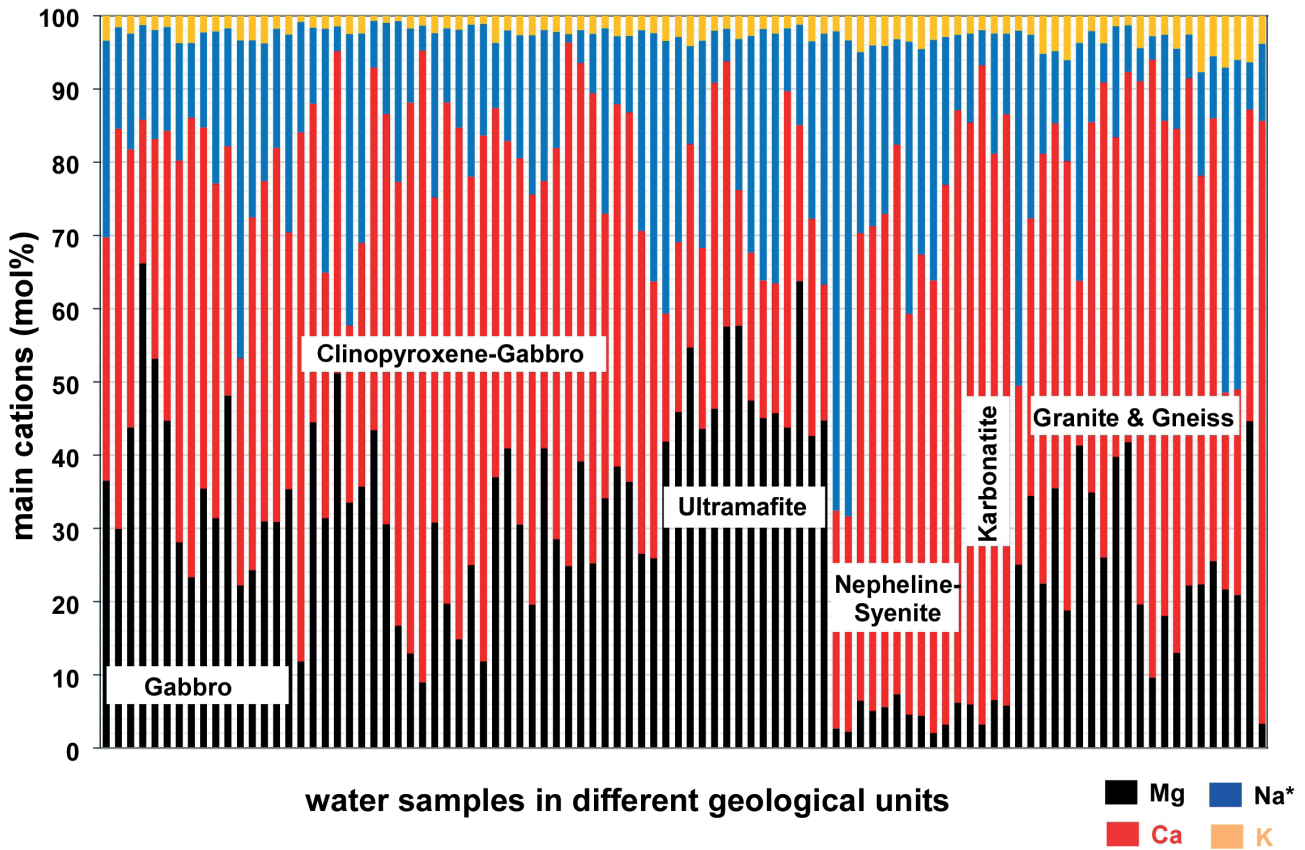


Figure 7. Relative cation distribution in the water samples. Na is reduced by the marine component ( $\text{Na}^*$ ).

quality. The Na/Cl ratio of all surface and subsurface water samples is equal to or higher than in the seawater samples ( $\text{Na}/\text{Cl} = 0.8$ ). The highest Na/Cl ratios are from waters collected in the nepheline-syenite mine (W31, W32, W39). High values are also found in waters circulating in ultramafic rocks (e.g., W20; Fig. 6).

Thus, the source of chloride in the collected, fast-circulating water samples is marine, as a result of the marine component in rainwater and the influence from blown spray from the sea. Sodium, on the other hand, has both a marine component ( $\text{Na}/\text{Cl} = 0.8$ ) and a 'rock' component ( $\text{Na}/\text{Cl} > 0.8$ ), deriving from alteration processes that have affected the rocks. Note: Na/Cl (mol-basis) of all surface waters and groundwater is  $> 0.8$  (Fig. 6).

Taking into account that parts of the Na concentrations measured in the water samples are of direct marine origin, Ca or Ca + Mg are the main cations in nearly all collected waters, even in samples from norites and syeno-gabbros (Fig. 4G, F). By neglecting the marine component of the sodium, the alkaline earth metals (Ca + Mg) in most water-samples of the Seiland Igneous Province are the main cations (Fig. 7), with the exception of two samples from the deeper part of the nepheline-syenite mine (W31, W32).

Considering this marine influence, the main alteration

component of nepheline-syenite and carbonatite in water is calcium, whereas the content of magnesium is very low (Fig. 7). The high calcium component in the nepheline-syenite waters is most probably caused by the presence of carbonatite vein intrusions and/or calcite-rich mafic dykes in the nepheline-syenite, as observed during fieldwork and described by Bruland (1980) and Gautneb (2009). Water samples from ultramafic rocks show a very high magnesium component (central part in Fig. 7). In gabbros, including clinopyroxene-, olivine- and syeno-gabbros, and norites, calcium or the earth alkali (Ca + Mg) dominate the water-type (left side of Fig. 7). The right-hand side of Fig. 7 shows the cation distribution of waters circulating in gneisses and granites nearby and outside the Seiland Igneous Province.

#### Waters in carbonatites and in the nepheline-syenite mine

Taking into account the marine influence on all water samples of the Seiland Igneous Province, the subsequent investigations on water-rock interaction are based on the hydrochemical data reduced by the marine component.

The dominating water-rock reaction in carbonatites is given by calcite (eq. 5), as a result of its relatively high dissolution rate and frequency in the rocks.

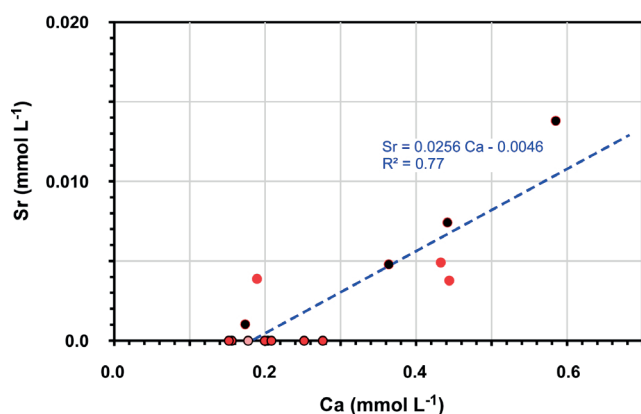
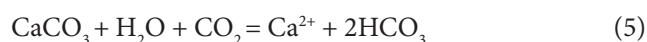


Figure 8. Correlation between Ca and Sr in carbonatite (black dots) and nepheline-syenite (red dots – within the mine, light red dot – spring waters). Detection limit of Sr is  $50 \mu\text{g L}^{-1}$ .



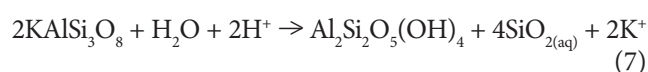
The influence on water chemistry according to the alteration of other mineral components like biotite, amphibole or apatite is much smaller (e.g., Lasaga et al., 1994). Thus, the magnesium concentration as a result of the alteration of biotite and amphibole is very low (Figs. 4F & 7) and phosphor, with apatite as possible source, is below the detection limit (Table 2B).

By reason of the generally relatively low TDS in all collected water samples, strontium could only be detected in higher concentrated waters, like the carbonatite and the nepheline-syenite waters (Table 2B). There seems to be a correlation between Ca and Sr (Fig. 8). This correlation is probably caused by the alteration of the primary SrO-rich calcite in the carbonatite and in the carbonatite veins of the nepheline-syenite and calcite-rich mafic dykes with high strontium concentrations, as described above. The slope of the correlation line in Fig. 8 with  $m = 0.0256$  corresponds to the SrO content of about 2 wt.% in the primary calcite phase, described by Jendryszczyk (2013).

Bruland (1980) studied recent near-surface weathering effects as a consequence of precipitation in alteration zones of **nepheline-syenites** and found that there is no difference in appearance between the alteration products of nepheline and K-feldspar. Dorfman (1958) and Bruland (1980) stated that the alteration of nepheline-syenite is a process of several stages. Bruland (1980), in addition, investigated the whole-rock composition of alteration products from alteration zones in the nepheline-syenite and found illite/hydromuscovite with a  $\text{K}_2\text{O}$  concentration of up to 9.7%. These alteration products are normally associated with low-grade metamorphism. However, Geis (1979) found that in the alteration zones in the nepheline-syenite, nepheline was replaced by zeolite aggregates. Li (2013) observed

in thin-sections the albitisation of nepheline. She also found a co-precipitate of calcite with thomsonite ( $\text{Ca}_2\text{NaAl}_5\text{Si}_5\text{O}_{20} \cdot 6\text{H}_2\text{O}$ ). Nonetheless, this process needs a Ca- and  $\text{HCO}_3^-$ -rich fluid, deriving probably from the carbonatite veins in the nepheline-syenite.

According to the findings of Bruland (1980) and by reason of the general investigations of Lasaga et al. (1994), Froger & Schweda (1998) and Zhou (2010), relatively high dissolution rates are expected of nepheline and significantly lower of K-feldspar. Generally, possible simplified reaction-equations of water-rock interaction (WRI) for waters within the mine are the dissolution of the end-member nepheline and K-feldspar, both forming kaolinite (eq. 6, 7).



Both reactions are consuming  $\text{H}^+$ , leading to an increase in the pH value. The theoretical considerations are corresponding with the measurements; all water samples collected in nepheline-syenite rocks within the mine had elevated pH values of up to 9.36 (Table 2B).

The whole-rock analyses of the nepheline-syenite (Table 1) showed Na/K ratios (mol-basis) of about 1.36, whereas in the collected water samples (Table 2B) in most cases  $\text{Na}^*/\text{K}$  is roughly about 10 and sometimes even higher ( $\text{Na}^*$  corresponds to Na, reduced by the marine component). Nepheline has a Na/K ratio of about 3.95, whereas in the K-feldspars the Na/K ratio is difficult to determine on account of the observed Na- and K-rich lamella texture. The nepheline-syenite contains about 40% K-feldspar and 35% nepheline. Since the molar mass of K-feldspar at 278.33 g/mol is much higher compared to that of nepheline, 142.05 g/mol, the Na/K ratio of K-feldspar is in the order of 0.85. Thus, in order to get  $\text{Na}^*/\text{K} = 10$  in the water, an additional K-sink is needed, i.e., a precipitation of K-rich mineral(s). However, the required K-sink could not be identified.

Thus, the sodium-potassium ratio is one of the most fundamental relationships in the nepheline-syenite waters. The  $\text{Na}^*$ -K stability diagram (Fig. 9) shows the dependency of the  $\text{Na}^*$ - and K-activity dependent on pH (expressed as  $\text{H}^+$ ) at 15°C. The calculation has been made for two saturation states of quartz ( $\text{SI}_{\text{Qtz}} = 0.0, -0.5$ ). Taking into account an assumed undersaturation of the nepheline-syenite waters with respect to quartz by reason of the  $\text{SiO}_2$ -poor nepheline, the collected water samples plot into the kaolinite window. Independent of the degree of undersaturation with respect to quartz, even highly developed waters will not plot in the muscovite window (Fig. 9).

The water data can be fitted to one continuous linear trend line with a slope of  $m = 1$  (violet dotted line

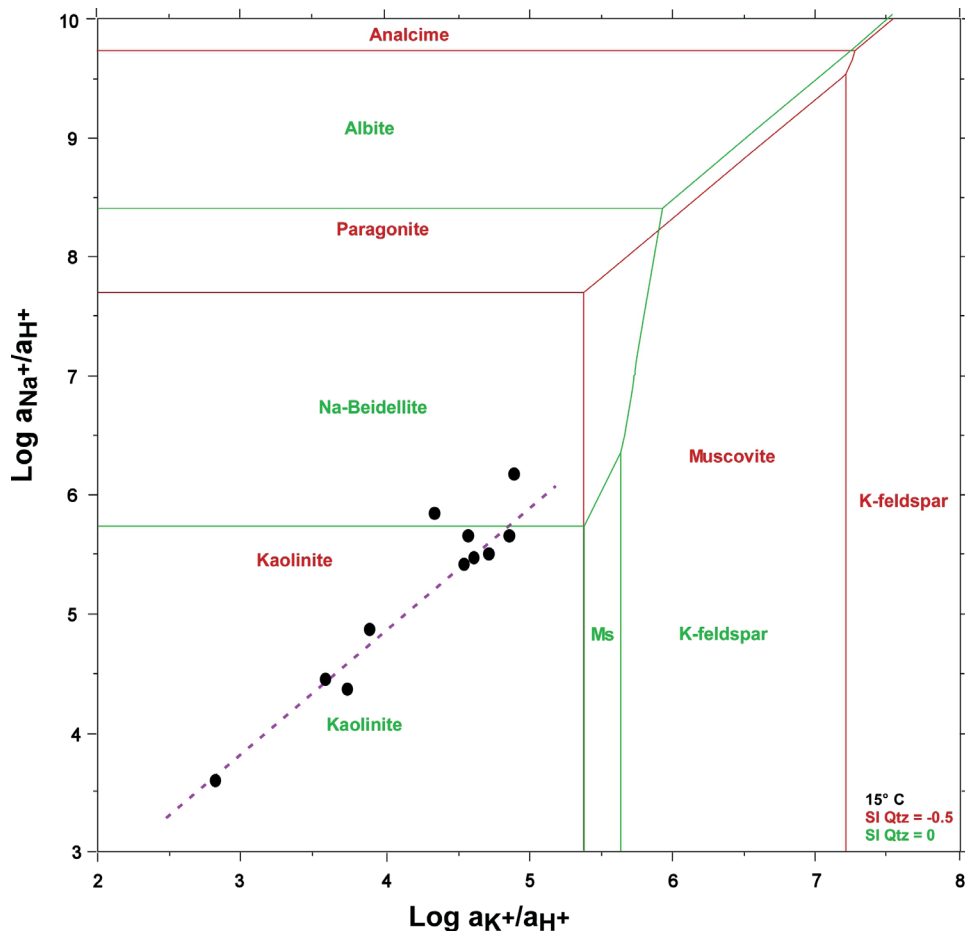


**Figure 9.** Stability diagram of K vs. Na\* activity of 'nepheline-syenite' waters (Table 2B) in dependency of pH for 15°C, atmospheric pressure and different saturation states of quartz, calculated with the thermodynamic program MacIIPTax (Brown et al., 1989) on the basis of thermodynamic data of Helgeson et al. (1981), Berman (1988), Liou et al. (1991) and the phase plotter of Lieberman (1991). The two different saturation states of quartz (0.0, -0.5) correspond to the chalcedony saturation states -0.28, -0.78.

in Fig. 9). Thus, waters will develop along this line, a parallel to the metastable extension of the paragonite-muscovite phase boundary, until saturation with respect to muscovite is achieved (paragonite is a sodium mica, with indicative formula  $\text{NaAl}_2[(\text{OH})_2\text{AlSi}_3\text{O}_{10}]$ , related to muscovite). They will then evolve along this vertical phase boundary also until saturation to paragonite is reached.

Similar studies regarding the incongruent dissolution of feldspars as well as irreversible reactions involving minerals and aqueous solutions were carried out by Helgeson (1974) and Helgeson et al. (1968).

### Waters in gabbro and ultramafic rock catchments

Analyses of rock samples have shown, as described above, that the main components of the gabbro samples are Ca- and Mg-rich clinopyroxene and plagioclase with a generally higher An than Ab component. Small amounts of orthopyroxene may also be present. Additionally, minor amounts of Ca-amphibole and Mg-rich olivine

may occur, the latter preferentially in olivine-gabbros. Typical for the ultramafic rocks are the high Mg and Fe but low K and  $\text{SiO}_2$  contents and that the rocks contain hardly any Ca-rich plagioclase.

Thus, waters collected in gabbros are expected to be either Ca-dominated or Mg-dominated, or a combination of both, the latter depending essentially on the olivine content of the gabbros in the catchment. Waters collected in ultramafic rocks should have – in consequence of the mafic minerals in the rocks – significantly higher Mg and lower Ca concentrations than waters circulating in a gabbro terrain. These common assumptions correspond to the hydrochemical composition of the water samples collected in gabbro- and ultramafic rock catchments.

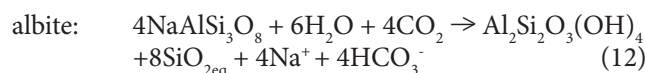
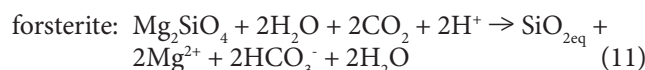
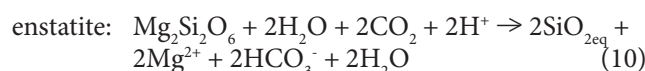
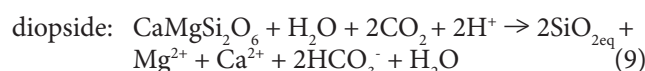
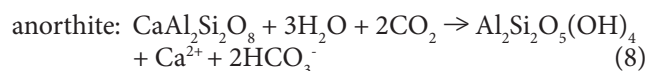
Fig. 10 shows the strong correlation between  $\text{TDS}^*$  and the (Ca + Mg) concentration in these water samples, whereas waters from gabbro catchments generally show somewhat higher Ca and somewhat lower Mg concentrations than waters from ultramafic rock catchments. Please note that the  $\text{TDS}^*$  is reduced by the marine Na and Cl components, as described above.

The mineralogical composition of the rock samples has shown that the *plagioclases* in the gabbros are generally Ca-rich, i.e., the An component ( $\text{CaAl}_2\text{Si}_2\text{O}_8$ ) is relatively high ( $\text{Ca}/(\text{Ca} + \text{Na})_{\text{pgl}} = 55$  to 100 vol.%). The *pyroxenes* in the gabbros could be classified as clinopyroxenes ((Mg, Fe)  $\text{CaSi}_2\text{O}_6$ ) and in the ultramafic rocks additionally as orthopyroxenes. The cation proportions (expressed as Wo, En, Fs), presented in the chapter on rock analyses, were used to calculate the diopside (Di), enstatite (En), ferrosilite (Fs) and hedenbergite (Hd) components of the clinopyroxenes. Thus, the average Di component ( $\text{CaMgSi}_2\text{O}_6$ ) is 80–87 mol.% and the En component ( $\text{Mg}_2\text{Si}_2\text{O}_6$ ) 3–10 mol.%. The majority of the *olivines* are Mg-rich, i.e., forsterites ( $\text{Mg}_2\text{SiO}_4$ ), and the *amphiboles* are Ca-rich.

According to Lasaga et al. (1994), Froger & Schweda (1998) and Zhou (2010), high dissolution rates are expected from anorthite, followed by forsterite, then enstatite and diopside, and with lower rates probably from albite and amphibole. So, taking also into account the frequency of occurrence of the specific mineral components, the most important and dominant alteration reaction in the gabbros is expected to be that of the anorthite component of plagioclase (eq. 8), followed by clinopyroxene (diopside, eq. 9) then orthopyroxene (enstatite, eq. 10). In olivine-rich gabbros the alteration reaction of olivine (eq. 11) could dominate the reactions described with eq. 9 and/or eq. 10. Because of the relative low Ab component in

plagioclase and its low dissolution rate in comparison to An (e.g., Lasaga et al., 1994), the alteration of the albite component (eq. 12) should not influence the water signature in the gabbros to any great extent. In ultramafic rocks, the predominant water-rock interaction (WRI) is expected to be the weathering of olivine (forsterite, eq. 11) and clinopyroxene (diopside, eq. 9), followed by that of orthopyroxene (enstatite, eq. 10).

Possible WRI equations in surface waters (eq. 8 and 12 from Stober & Bucher, 1999b):



with:  $\text{Al}_2\text{Si}_2\text{O}_5(\text{OH})_4$  – kaolinite,  $\text{SiO}_{2\text{eq}}$  – silica in water

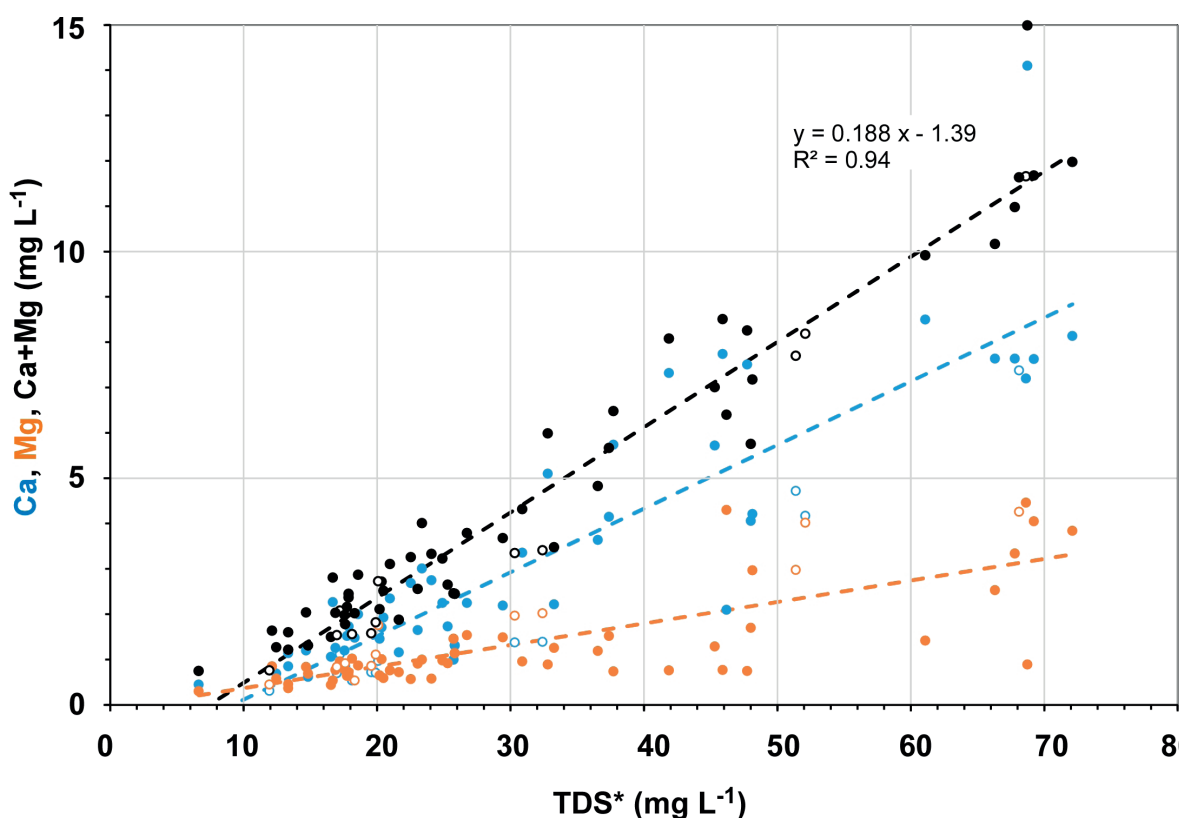


Figure 10. TDS\* vs. the calcium concentration, magnesium concentration and the sum of both (Ca + Mg) in gabbro (filled symbols) and ultramafic rock catchments (hollow symbols). TDS\* is reduced by the marine component (Na, Cl).

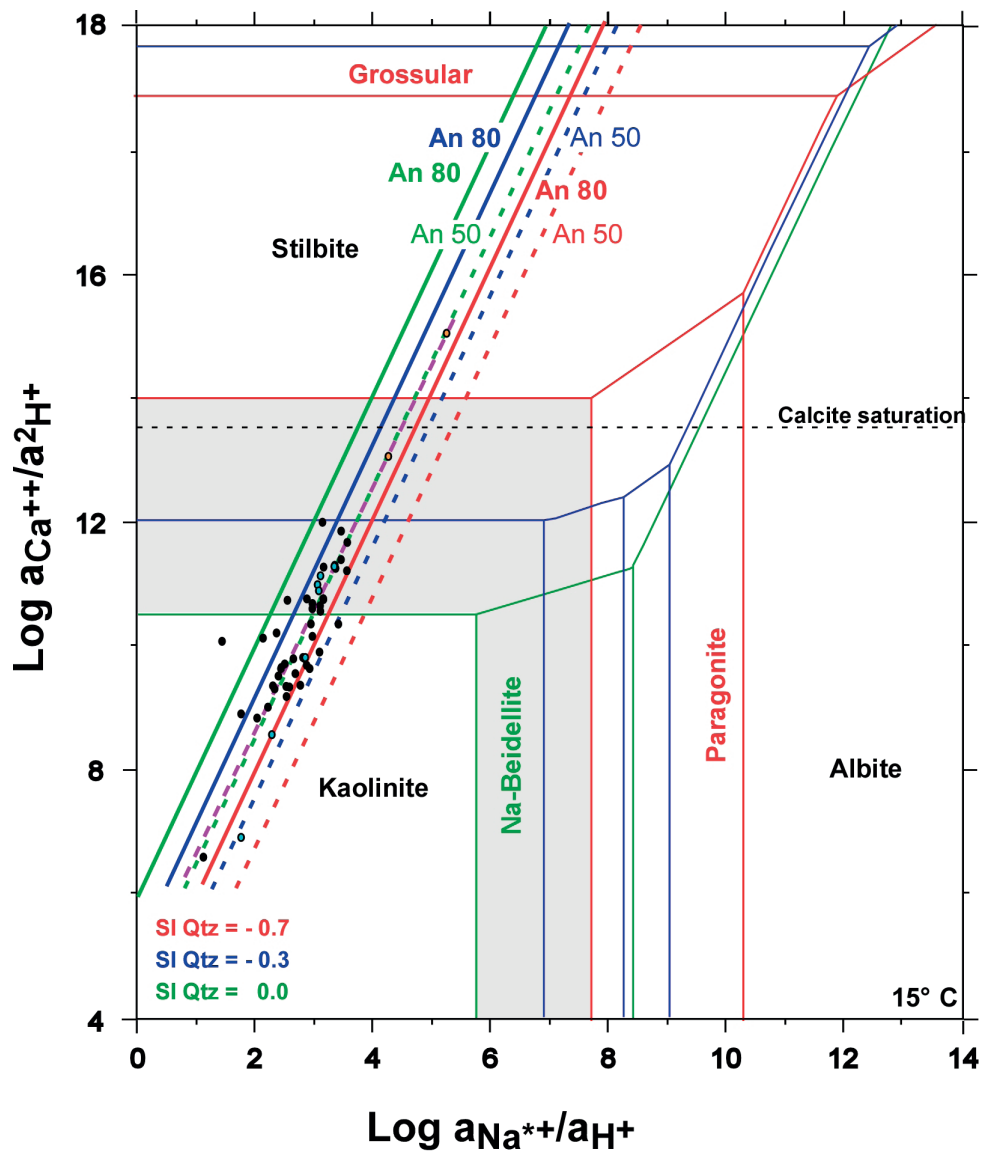


Figure 11. Stability diagram of  $\text{Na}^+$  vs.  $\text{Ca}$  activity of 'gabbro' waters (Table 2C; black dots – brooks, turquoise – talus, pink – tunnel) in dependency of pH for 15°C, atmospheric pressure and different saturation states of quartz, calculated with the thermodynamic program MacIIPTax (Brown et al., 1989) on the basis of thermodynamic data of Helgeson et al. (1981), Berman (1988), Liou et al. (1991) and the phase plotter of Lieberman (1991). The three different saturation states of quartz correspond to the chalcedony saturation states -0.28, -0.58, -0.78. Calcite saturation according to PHREEQC (Parkhurst & Appelo, 1999)

These simplified considerations suggest that the  $\text{Ca}$  concentrations in waters collected in gabbros should generally be higher than the  $\text{Mg}$  concentrations and that the  $\text{Na}$  concentrations should be generally very low, whereas in ultramafic rocks relatively high  $\text{Mg}$  concentrations in the water are to be expected, but with a certain amount of  $\text{Ca}$  too. That is precisely what is observed in the analysed waters (Figs. 7 & 10). All reactions (eq. 8–12) lead to  $\text{HCO}_3^-$  as the dominant anion, as measured in the water samples. However, a significant increase of pH with increasing TDS in consequence of the 'minor important' reactions (eq. 9–11) was not detectable, neither in the gabbro nor in the ultramafic rock waters. All surface-water samples showed circumneutral pH. On the other hand, the two subsurface gabbro-water samples from the Øksfjordtunnel (W5,

W99) had significantly elevated pH-values (9.39, 8.40), demonstrating proton-consuming reactions, since the atmospheric  $\text{CO}_2$  inside the mountain is consumed by near-surface WRI reactions.

During the alteration process in gabbros,  $\text{H}_2\text{O}$  is continuously withdrawn from the water according to eq. 8 (main important alteration reaction) leading to an increase in TDS and, thus, in the long term following Fig. 11 theoretically to the formation of stilbite, a  $\text{Na}/\text{Ca}$  zeolite mineral (occurring in both sodium- and calcium-rich forms) binding free  $\text{H}_2\text{O}$  into the structure.

Water composition in gabbro terrains indicates that dissolution of the major minerals,  $\text{Ca}$ -rich plagioclase and clinopyroxene (also in some olivine-rich localities

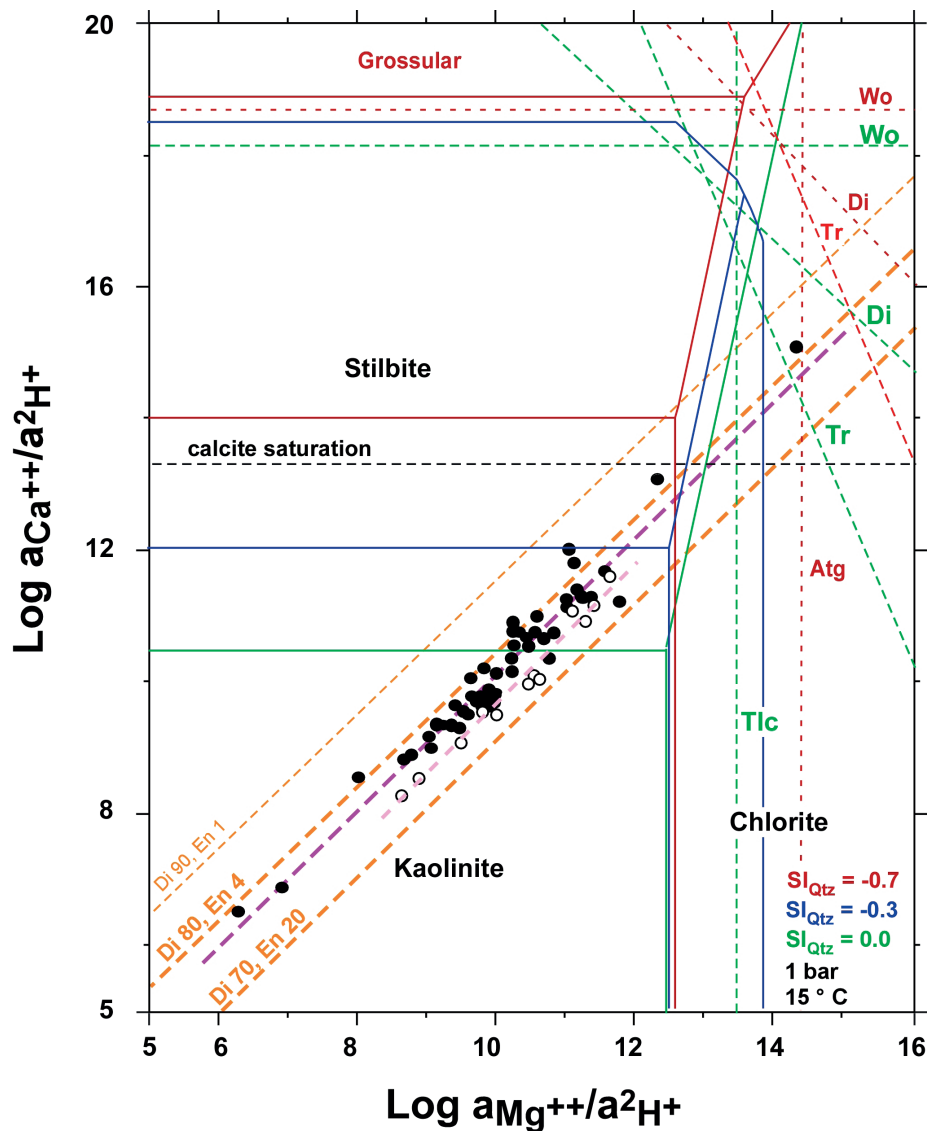


Figure 12. Stability diagram of Mg- vs. Ca-activity of waters in gabbro (Table 2C; black dots) and ultramafic rocks (Table 2D; hollow dots) in dependency of pH for 15°C, atmospheric pressure and different saturation states of quartz, calculated with the thermodynamic program MacIIptax (Brown et al., 1989) on the basis of thermodynamic data of Helgeson et al. (1981), Berman (1988), Liou et al. (1991) and the phase plotter of Lieberman (1991). The three different saturation states of quartz correspond to the chalcedony saturation states -0.28, -0.58, -0.78. Calcite saturation according to PHREEQC (Parkhurst & Appelo, 1999).

forsterite), essentially dominates the chemical evolution of the waters and that the reaction with the gabbro rock matrix is the major source of the cations. Accordingly, plagioclase with its An and Ab components is expected to supply Ca and Na and clinopyroxene to contribute Mg and Ca, and in olivine-rich gabbros an additional Mg input is assumed.

In ultramafic rocks, olivine and clinopyroxene (and to some degree orthopyroxene) are expected to be the dominating factors enhancing Mg and Ca in the waters.

Many aspects of the water composition and evolution will be better understood by utilising isobaric and isothermal activity diagrams of the phase relationships in the composition space of particular interest. In gabbro

waters, the calcium-sodium and the calcium-magnesium relationships are the fundamental ties, whereas in waters circulating in ultramafic rocks the calcium-magnesium relationship is the most important.

The Ca-Na\* stability diagram (Fig. 11) shows the dependency of the Ca and Na\* activity dependent on pH (expressed as H<sup>+</sup>) at 15°C. Taking into account the assumed undersaturation of the gabbro-waters with respect to quartz, the water samples plot into the kaolinite window, depending on the degree of undersaturation. The calculation has been done for several saturation states of quartz (SI<sub>Qtz</sub> = 0.0, -0.3, -0.7).

The gabbro water data can be fitted to one continuous linear trend (violet dotted line in Fig. 11) with a slope of

$m = 2$ , given as a result of the alteration of plagioclase (An and Ab components). Thus, waters in a pure plagioclase terrain will develop along the An–Ab line until saturation with respect to stilbite is reached, and then follow along this stable phase-boundary until saturation with respect to paragonite or – depending on the saturation state of quartz – Na-beidellite is reached. Expressed as  $X_{An}$  (Ca/(Ca + Na)), the gabbro waters are close to  $X_{An} = 0.70$  and thus in between An 50 and An 80 on an activity basis. The best fit is achieved for an assumed saturation state of quartz  $SI_{Qtz} = -0.3$  (Fig. 11). Thus, saturation with respect to calcite will not be reached (Fig. 11). All water samples plot in the kaolinite field, with the exception of two samples collected in the Øksfjordtunnel which have different boundary conditions.

Equivalent investigations with the Mg and Ca activity (dependent on pH, expressed as  $H^+$ ) at 15°C show a strong relationship between calcium and magnesium for waters in gabbro and in ultramafic rocks, respectively (Fig. 12). The calculation has been done for different saturation states of quartz:  $SI_{Qtz} = 0.0$ ,  $SI_{Qtz} = -0.3$  and  $SI_{Qtz} = -0.7$ . The data of the gabbro and the ultramafic waters follow a trend-line with a slope  $m = 1$  in the Mg–Ca stability diagram (violet dotted lines in Fig. 12). Taking into account the assumed undersaturation of the waters with respect to quartz ( $SI_{Qtz} \approx -0.3$ ), all collected water samples – with exception of the two gabbro-samples collected in the Øksfjordtunnel – plot into the kaolinite field of this diagram (Fig. 12). Waters in a pure clinopyroxene rock will develop along the Di–En line until saturation with respect to stilbite is reached, and then follow along this stable phase-boundary until they are saturated with respect to chlorite. Assuming  $SI_{Qtz} = -0.3$ , saturation with respect to calcite will not be achieved. Expressed as diopside ( $CaMg[Si_2O_6]$ ) and enstatite ( $Mg_2Si_2O_6$ ) components, all gabbro and ultramafic rock waters lie in a small clinopyroxene-controlled band between Di 70 En 20 and Di 90 En 1 (orange dotted lines in Fig. 12), whereas the Di/En ratio in gabbro waters is higher than in ultramafic rock waters.

Thus, olivine (i.e., forsterite), respectively orthopyroxene, does not control the water chemistry in the gabbros, respectively in the ultramafic rocks, to any significant extent, because otherwise the data would follow a trend-line with a slope of  $m = 2$ , getting saturated with respect to chlorite. Consequently, in both catchments magnesium is derived mainly from clinopyroxene.

Thus, plagioclase and clinopyroxene control the hydrochemistry in gabbro-dominated terrains and in ultramafic rocks clinopyroxene is controlling the chemistry of the waters.

## Waters in granite and gneiss catchments

Waters collected in granite and gneiss catchments are generally poorly mineralised (Stober, 1995; Frengstad, 2002; Frengstad & Banks, 2007). Thus, the water samples in the investigation area had very low TDS too, especially under the arctic climatic conditions. Waters in gneiss- and granite-dominated terrains belong to the waters having basically the lowest TDS of all sampled waters. Neglecting the marine influence, the water type is dominated by Ca and/or  $Na^+$  (Na reduced by the marine component) and by  $HCO_3^-$  (Figs. 4H, 5 & 7). Water chemistry in granite and gneiss catchments is mainly influenced by the alteration of plagioclase, whereas the water type is dependent on the An/Ab ratio in the plagioclase (Bucher & Stober, 2000; Banks & Frengstad, 2006). In the gneisses the water type is thus Ca-dominated, whereas in the granites preferentially Na-dominated.

## Conclusions

During two research campaigns, water and rock samples were collected in the Seiland Igneous Province, North Norway. The focus of the sampling was on silicate rocks which are easily weathered such as nepheline-syenites, carbonatites, ultramafic rocks and gabbros. Fieldwork comprised a detailed field study of selected outcrops. Care was taken to collect water samples in defined catchments with the same lithology. For comparison reasons, also water samples in granites and gneisses were collected. Precipitation and sea-water was also collected as reference material for the field study in view of possible influences in consequence of rainfall and sea spray. Field observations, geochemical compositions of the different rock samples, and chemical analyses of the collected water samples are used to model the interaction of water (rainwater) with unstable (easily) weatherable silicate rocks, to better understand silicate weathering processes in general.

In this paper, the hydrochemistry in different crystalline basement rocks of the Seiland Igneous Province were studied. The focus was on relatively fast-weathering rock processes visible in the hydrochemical properties of surface water and groundwater. Thus, first of all the mineralogical and geochemical compositions of the different rock types were investigated: nepheline-syenite, carbonatite, gabbro and ultramafic rocks. Knowing the different components of each rock-type, the main components (minerals) responsible for the water chemistry could be identified. The hydrochemical properties of the diverse (rock-specific) catchments differ from each other. All collected waters had relatively low TDS, between  $7 \text{ mg L}^{-1}$  and  $118 \text{ mg L}^{-1}$ . To carry out further hydrochemical investigations, the marine

influence in the water samples, represented by sea spray or rainfall, had to be eliminated.

All waters are undersaturated with respect to quartz. Water chemistry in a carbonatite-dominated terrain is regulated by the weathering process of calcite. In nepheline-syenite, the sodium-potassium ratio is one of the fundamental relationships, because of the nepheline and K-feldspar components of nepheline-syenite. The chemical development of rainwater in different lithologies could be shown and explained with the aid of mineral stability diagrams.

The investigations of Gascoyne & Kamineni (1993) on groundwater in a gabbro/anorthosite complex in Massey, Ontario (Canada), showed a Ca-Na-HCO<sub>3</sub> water type with elevated Mg concentrations, a slightly elevated pH value and TDS of 150 mg L<sup>-1</sup>. The authors could show that the waters plot into the stability field of kaolinite, as do the waters analysed in this investigation. With increasing depth, i.e., prolonged residence time, Gascoyne & Kamineni (1993) observed that the water type changed into a Na-HCO<sub>3</sub> water with higher TDS and pH values. Since the residence times of the investigated surface waters and shallow groundwaters are much shorter, the TDS in the Seiland gabbro waters are less and more strongly dominated by Ca and Mg. On the other hand, with increasing residence time and contact area for water on rock-surfaces, i.e., waters in talus material or in tunnels, these waters showed slightly elevated TDS and pH. Thus, the investigations of Gascoyne & Kamineni (1993) are in good agreement with our results.

In contrast to our findings in North Norway, Marques et al. (2008) presented hydrochemical properties of surface water with much higher TDS (850 mg L<sup>-1</sup>). The investigated brook is flowing through ultramafic rocks, dunites, in Central Portugal. While the dominating ions are the same as in the ultramafic rock catchments of Seiland, Mg and HCO<sub>3</sub>, the brook water in Central Portugal has a significantly elevated pH. The pH values of our samples in ultramafic rocks are circumneutral (6.65–7.69), whereas the waters sampled in the ultramafic talus material showed a pH in the upper portion of this range. Concerning the general setting in the investigated area of Marques et al. (2008), with a lot of upwelling highly concentrated waters from diverse depths in the entire area and near the brook, it was assumed that the chemistry of the brook water might be influenced by nearby upwelling springs, mixing with the brook water. Quite possibly the more favourable climatic conditions for weathering in Central Portugal have helped to intensify the alteration process and thus increase TDS (and pH) in the water.

Equivalent investigations were carried out by Barnes et al. (1967) and Barnes & O'Neil (1969) on surface waters and shallow groundwaters in serpentinites, peridotites and dunites in the western United States (California,

Oregon). The waters showed TDS values even up to 1.500 mg L<sup>-1</sup> with Mg and HCO<sub>3</sub> as dominant ions and a pH up to 8.9.

The investigations of Bucher et al. (2015) in surface waters of the Ronda peridotite, southern Spain, also showed relatively high TDS (275–563 mg L<sup>-1</sup>) and elevated pH values (8.36–8.54). In all waters Mg and HCO<sub>3</sub> were also the dominant ions. The hydrochemistry of the waters develops when atmospheric carbon dioxide dissolves in the water and forms bicarbonate, as olivine and serpentine minerals in the near-surface react with the waters and release magnesium ions and silica.

Zhou (2010), on the other hand, carried out investigations in brook waters in serpentinite and peridotite catchments in the high alpine area of Zermatt-Saas, Switzerland. The climatic conditions there are more or less similar to those of our area in northern Norway. The waters that Zhou (2010) collected are very poorly mineralised with average TDS of 21 mg L<sup>-1</sup>. Her water samples also showed Mg and HCO<sub>3</sub> as the dominating ions, and pH values are in most cases slightly elevated. She found that with increasing TDS SiO<sub>2</sub>, Na and K are progressively increasing and assumed that these waters are originating predominantly from Mg-silicates as exposed in rocks in the catchment.

Drever & Zobrist (1992) studied indirectly the climatic effect on the weathering process and surface-water composition by investigating the weathering process as a function of elevation in the southern Swiss Alps. They found a more or less exponential decrease of the weathering effect on water chemistry with increasing elevation. Their findings can explain the generally surprisingly low TDS of the water samples in relatively fast-weathering rocks of the Seiland Igneous Province in North Norway under arctic climatic conditions.

Further investigations will focus on deep-seated waters, from tunnels and wells, especially in gabbro- and ultramafic rock-dominated terrains. These waters should have longer residence times in the subsurface and are thus more highly developed than surface waters. It is planned to compare the hydrochemistry of these waters with the results presented in the stability diagrams. Thus, we also intend to sample alteration products of the various rock types. In addition, a detailed isotopic investigation of groundwater is planned in order to provide information concerning the age and origin of the collected waters.

**Acknowledgements.** We would like to thank Northcape Minerals AS, for the possibility to carry out investigations within the nepheline-syenite mine. We thank Sigrid Hirth-Walther and Isolde Schmidt for laboratory assistance. The Rinne Foundation appreciatively supported the field-work. We would like to thank two reviewers, David Banks and an anonymous reviewer, for helping to improve the manuscript considerably. We also thank Trond Slagstad for suggestions and editorial work.

## References

- Anderson, G.M. 1996: *Thermodynamics of Natural Systems*. John Wiley & Sons, New York, 382 pp.
- Aquilina, L., Sureau, J.F. & Steinberg, M. 1997: Comparison of surface-, aquifer- and pore-waters from a Mesozoic basin and its underlying Paleozoic basement, southeast France: Chemical evolution of waters and relationships between aquifers. *Chemical Geology* 138, 185–209. [https://doi.org/10.1016/S0009-2541\(97\)00011-9](https://doi.org/10.1016/S0009-2541(97)00011-9).
- Banks, D. & Frengstad, B. 2006: Evolution of groundwater chemical composition by plagioclase hydrolysis in Norwegian anorthosites. *Geochimica et Cosmochimica Acta* 70, 1337–1355. <https://doi.org/10.1016/j.gca.2005.11.025>.
- Barnes, I., LaMarche, V.C. Jr. & Himmelsberg, G.R. 1967: Geochemical evidence of present-day serpentinization. *Science* 56, 830–832. <https://doi.org/10.1126/science.156.3776.830>.
- Barnes, I. & O'Neil, J.R. 1969: The Relationship between Fluids in Some Fresh Alpine-Type Ultramafics and Possible Modern Serpentinization, Western United States. *Geological Society of America Bulletin* 80, 1947–1960. [https://doi.org/10.1130/0016-7606\(1969\)80\[1947:TRBFIS\]2.0.CO;2](https://doi.org/10.1130/0016-7606(1969)80[1947:TRBFIS]2.0.CO;2).
- Barnes, I., O'Neil, J.R. & Trescases, J.J. 1978: Present day serpentinization in New Caledonia, Oman and Yugoslavia. *Geochimica et Cosmochimica Acta* 42, 144–145. [https://doi.org/10.1016/0016-7037\(78\)90225-9](https://doi.org/10.1016/0016-7037(78)90225-9).
- Bennett, M.C. 1974: The emplacement of a high temperature peridotite in the Seiland province of the Norwegian Caledonides. *Journal of the Geological Society of London* 130, 205–228. <https://doi.org/10.1144/gsjgs.130.3.0205>.
- Berman, R.G. 1988: Internally-Consistent Thermodynamic Data for Minerals in the System: Na<sub>2</sub>O- K<sub>2</sub>O- CaO- MgO- FeO- Fe<sub>2</sub>O<sub>3</sub>- Al<sub>2</sub>O<sub>3</sub>- SiO<sub>2</sub>- TiO<sub>2</sub>- H<sub>2</sub>O- CO<sub>2</sub>. *Journal of Petrology* 29, 445–522. <https://doi.org/10.1093/petrology/29.2.445>.
- Braitsch, O. & Herrmann, A.G. 1963: Zur Geochemie des Broms in salinaren Sedimenten, Teil I. *Geochimica et Cosmochimica Acta* 27, 361–391. [https://doi.org/10.1016/0016-7037\(63\)90077-2](https://doi.org/10.1016/0016-7037(63)90077-2).
- Brown, G.H., Berman, R.G. & Perkins, E.H. 1989: PTA-SYSTEM; a GeO-Calc software package for the calculation and display of activity-temperature-pressure phase diagrams. *American Mineralogist* 74, 485–487.
- Brown, G.H., Sharp, M.J., Tranter, M., Gurnell, A.M. & Nienow, P.W. 1994: Impact of Post-Mixing Chemical-Reactions on the Major Ion Chemistry of Bulk Meltwaters Draining the Haut Glacier Darolla, Valais, Switzerland. *Hydrology Processes* 8, 465–480. <https://doi.org/10.1002/hyp.3360080509>.
- Bruland, T. 1980: *Lillebukt alkaline complex: Mafic dykes and alteration zones in Nabberen nepheline syenite*. PhD thesis, University of Bergen, 231 pp.
- Bucher, K. 1991: Mantle fragments in the Scandinavian Caledonides. *Tectonophysics* 190, 173–192. [https://doi.org/10.1016/0040-1951\(91\)90429-V](https://doi.org/10.1016/0040-1951(91)90429-V).
- Bucher, K. & Stober, I. 2000: Hydrochemistry of water in the crystalline basement. In Stober, I. & Bucher, K. (eds.): *Hydrogeology of Crystalline Rocks*, Kluwer Academic Publishers, Dordrecht, pp. 141–175. [https://doi.org/10.1007/978-94-017-1816-5\\_7](https://doi.org/10.1007/978-94-017-1816-5_7).
- Bucher, K. & Stober, I. 2001: Does plagioclase control the composition of groundwater in crystalline basement. In Cidu, R. (ed.): *WRI*, A.A. Balkema, Lisse, pp. 149–152.
- Bucher, K., Stober, I. & Müller-Sigmund, H. 2015: Weathering crusts on peridotite. *Contributions to Mineralogy and Petrology* 169:52, 1–15.
- Chavagnac, V., Monnin, C., Ceuleneer, G., Boulart, C. & Hoareau, G. 2013: Characterization of hyperalkaline fluids produced by low-temperature serpentinization of mantle peridotites in the Oman and Ligurian ophiolites. *Geochemistry Geophysics Geosystems* 14, 2496–2522. <https://doi.org/10.1002/ggge.20147>.
- Clark, I.D. & Fontes, J.-C. 1990: Paleoclimatic Reconstruction in Northern Oman based on Carbonates from Hyperalkaline Groundwaters. *Quaternary Research* 33, 320–336. [https://doi.org/10.1016/0033-5894\(90\)90059-T](https://doi.org/10.1016/0033-5894(90)90059-T).
- Dorfman, M.D. 1958: Geochemical characteristic of weathering processes in nepheline syenite of Khibina tundra. *Geochemistry, A Translation of Geokhimiya* 5, 537–555.
- Drever, J.I. 1997: *The Geochemistry of Natural Waters*. 3rd ed., Prentice Hall, Upper Saddle River, N.J., 436 pp.
- Drever, J.I. & Hurcomb, D.R. 1986: Neutralization of Atmospheric Acidity by Chemical-Weathering in an Alpine Drainage-Basin in the North Cascade Mountains. *Geology* 14, 221–224. [http://dx.doi.org/10.1130/0091-7613\(1986\)14<221:NOAABC>2.0.CO;2](http://dx.doi.org/10.1130/0091-7613(1986)14<221:NOAABC>2.0.CO;2).
- Drever, J.I. & Zobrist, J. 1992: Chemical-Weathering of Silicate Rocks as a Function of Elevation in the Southern Swiss Alps. *Geochimica et Cosmochimica Acta* 56, 3209–3216. [https://doi.org/10.1016/0016-7037\(92\)90298-W](https://doi.org/10.1016/0016-7037(92)90298-W).
- Frengstad, B. 2002: *Groundwater quality of crystalline bedrock aquifers in Norway*. PhD thesis, Norwegian University of Science and Technology, Trondheim, 389 pp.
- Frengstad, B. & Banks D. 2007: Universal controls on the evolution of groundwater chemistry in crystalline bedrock: The evidence from empirical and theoretical studies. In Krasny, J. & Sharp, J.M. (eds.): *Groundwater in Fractured Rocks*, Taylor & Francis/Balkema, Leiden, Netherlands, pp. 275–289. <https://doi.org/10.1201/9780203945650.ch18>.
- Frognier, P. & Schweda, P. 1998: Hornblende dissolution kinetics at 25°C. *Chemical Geology* 151, 169–179. [https://doi.org/10.1016/S0009-2541\(98\)00078-3](https://doi.org/10.1016/S0009-2541(98)00078-3).
- Gardner, P.M. 1980: The geology and petrology of the Hasvik gabbro, Sørøy, Northern Norway. PhD thesis, University of London, 423 pp.
- Garrels, R.M. & Mackenzie, F.T. 1971: Gregors Denudation of Continents. *Nature* 231, 382–383. <https://doi.org/10.1038/231382a0>.
- Gascoyne, M. & Kamini, D.C. 1993: The Hydrogeochemistry of Fractured Plutonic Rocks in the Canadian Shield. *Applied Hydrogeology* 2, 43–49. <https://doi.org/10.1007/s100400050044>.
- Gautneb, H. 2009: Review of the geology and the apatite distribution of the carbonatite in the Lillebukt Alkaline Complex, Stjernøy, Northern Norway. *Norges geologiske undersøkelse Report 2009.061*, 34 pp.
- Geis, H.P. 1979: Nepheline syenite on Stjernøy, Northern Norway. *Economic Geology* 74, 1286–1295. <https://doi.org/10.2113/gsecongeo.74.5.1286>.
- Griffin, W.L., Sturt, B.A., O'Neill, J.O., Kirkland, C.L. & O'Reilly, S.Y. 2013: Intrusion and contamination of high-temperature dunite magma: the Nordre Bumandsfjord pluton, Seiland, Arctic Norway. *Contributions to Mineralogy and Petrology* 165, 903–930. <https://doi.org/10.1007/s00410-012-0841-6>.
- Heier, K.S. 1961: Layered gabbro, hornblendite, carbonatite and nepheline syenite on Stjernøy, North Norway. *Norsk Geologisk Tidsskrift* 41, 109–155.
- Heim, M., Bleken, M.A., Gjengedal, E.L., Hillersøy, M.H. & Gautneb, H. 2010: The agrogeological potential of apatite-biotite-carbonatite (Stjernøy, Northern Norway) as slow release rock fertilizer. [http://www.borealagrominerals.com/uploads/2/2/1/4/2214955/norwegian\\_study.pdf](http://www.borealagrominerals.com/uploads/2/2/1/4/2214955/norwegian_study.pdf).
- Helgeson, H.C. 1974: Chemical interactions of feldspars and aqueous solutions. In McKenzie, W.S. & Zussmann, J. (eds.): *The feldspars*, Manchester University Press, Manchester, pp. 184–217.
- Helgeson, H.C., Garrels, R.M. & MacKenzie, F.T. 1968: Evaluation of irreversible reactions in geochemical processes involving minerals and aqueous solutions- II. Applications. *Geochimica et Cosmochimica Acta* 33, 455–481. [https://doi.org/10.1016/0016-7037\(69\)90127-6](https://doi.org/10.1016/0016-7037(69)90127-6).
- Helgeson, H.C., Kirkham, D.H. & Flowers, G.C. 1981: Theoretical prediction of the thermodynamic behaviour of aqueous electrolytes at high pressures and temperatures. IV. Calculation of activity coefficients, osmotic coefficients, and apparent molal and standard and relative partial molal properties to 600°C and 5 kb. *American Journal of Science* 281, 1249–1516. <https://doi.org/10.2475/ajs.281.10.1249>.

- Hilberg, S. & Riepler, F. 2016: Interaction of various flow systems in small alpine catchments: conceptual model of the upper Gurk Valley aquifer, Carinthia, Austria. *Hydrogeology Journal* 24, 1231–1244. <https://doi.org/10.1007/s10040-016-1396-9>.
- Hollocher, K. 2007: Calculation of a CIPW norm from a bulk chemical analysis. <http://www.union.edu/PUBLIC/GEODEPT/COURSES/ptrology/norms.htm>. Geology Department, Union College, Schenectady, NY, 12308, USA
- Jendryszczyk, N. 2013: *The Carbonatite of the Lillebukt Alkaline Complex on Stjernøya Island, Northern Norway*. MSc thesis, University of Freiburg, 129 pp.
- Kirkland, C.L., Daly, J.S., Chewc, D.M. & Page, L.M. 2008: The Finnmarkian Orogeny revisited: An isotopic investigation in eastern Finnmark, Arctic Norway. *Tectonophysics* 460, 158–177. <https://doi.org/10.1016/j.tecto.2008.08.001>.
- Lasaga, A.C. 1984: Chemical kinetics of water-rock interactions. *Journal of Geophysical Research* 89, 4009–4025. <https://doi.org/10.1029/JB089iB06p04009>.
- Lasaga, A.C. 1998: *Kinetic Theory in the Earth Sciences*. Princeton University Press, Princeton, New Jersey, 287 pp. <https://doi.org/10.1515/9781400864874>.
- Lasaga, A.C., Soler, J.M., Ganor, J., Burch, T.E. & Nagy, K.L. 1994: Chemical weathering rate laws and global geochemical cycles. *Geochimica et Cosmochimica Acta* 58, 2361–2386. [https://doi.org/10.1016/0016-7037\(94\)90016-7](https://doi.org/10.1016/0016-7037(94)90016-7).
- Leake, B.E., Woolley, A.R., Birch, W.D., Burke, E.A.J., Ferraris, G., Grice, J.D., Hawthorne, F.C., Kisch, H.J., Krivovichev, V.G., Schumacher, J.C., Stephenson, N.C.N. & Whittaker, E.J.W. 2004: Nomenclature of amphiboles: additions and revisions to the International Mineralogical Association's amphibole nomenclature. *Mineralogical Magazine* 68, 209–215. <https://doi.org/10.1180/0026461046810182>.
- Li, X. 2013: *Alkaline magmatism, water-rock interaction and multiple metamorphism in the Seiland Igneous Province, Northern Norway*. PhD thesis, University of Freiburg, 439 pp.
- Lieberman, J. 1991: *GridLoc v.1.3 a Phase Diagram Plotter*.
- Liou, J.G., de Capitani, C. & Frey, M. 1991: Zeolite equilibria in the system  $\text{CaAl}_2\text{Si}_2\text{O}_8\text{-NaAlSi}_3\text{O}_8\text{-SiO}_2\text{-H}_2\text{O}$ . *New Zealand Journal of Geology and Geophysics* 34, 293–301. <https://doi.org/10.1080/00288306.1991.9514467>.
- Marques, J.M., Carreira, P.M., Carvalho, M.R., Matias, M.J., Goff, F.E., Basto, M.J., Graca, R.C., Aires-Barros, L. & Rocha, L. 2008: Origins of high pH mineral waters from ultramafic rocks, Central Portugal. *Applied Geochemistry* 23, 3278–3289. <https://doi.org/10.1016/j.apgeochem.2008.06.029>.
- Menegon, L., Nasipuri, P., Stünitz, H., Behrens, H. & Ravna, E. 2011: Dry and strong quartz during deformation of the lower crust in the presence of melt. *Journal of Geophysical Research* 116, 1–23. <https://doi.org/10.1029/2011JB008371>.
- Miller, H.M., Matter, J.M., Kelemen, P., Ellison, E.T., Conrad, M.E., Fierer, N., Ruchala, T., Tominaga, M. & Templeton, A.S. 2016: Modern water/rock reactions in Oman hyperalkaline peridotite aquifers and implications for microbial habitability. *Geochimica et Cosmochimica Acta* 179, 217–241. <https://doi.org/10.1016/j.gca.2016.01.033>.
- Mjelde, Ø. 1983: *Geologi og Petrografi av Nabberen Nefelin-Syenitt og dens Forhold til de omliggende Syenitter, Nefelinsyenittgneis, Karbonatitt og Fenittiserte gabbroiske Bergarter i sydlige del av Lillebukt Alkaline Kompleks, Stjernøya*. Cand. scient. thesis, University of Bergen, 315 pp.
- Nordstrom, D.K., Plummer, L.N., Wigley, T.M.L., Wolery, T.J., Ball, J.W., Jenne, E.A., Bassett, R.L., Crerar, D.A., Florence, T.M., Fritz, B., Hoffman, M., Holdren Jr., G.R., Lafon, G.M., Mattigod, S.V., McDuff, R.E., Morel, F., Reddy, M.M., Sposito, G. & Thraillkill, J. 1979: A comparison of computerized chemical models for equilibrium calculations in aqueous systems. In Jenne, E.A. (ed.): *Chemical Modeling in Aqueous Systems*, American Chemical Society Symposium Series 93, American Chemical Society, Washington D.C., pp. 857–892. <https://doi.org/10.1021/bk-1979-0093.ch038>.
- Oosterom, M.G. 1963: The ultramafites and layered gabbro sequences in the granulite facies rocks on Stjernøya, Finnmark, Norway. *Leidse Geologiske Meddelelser* 28, 179–296.
- Parkhurst, D.L. & Appelo, C.A.J. 1999: PHREEQC (Version2) — a computer program for speciation, batch-reaction, one-dimensional transport, and inverse geochemical calculations. *US Geological Survey Water-Resources Investigation Report*, pp. 99–4259.
- Pedersen, R.B., Dunning, G.R., Robins, B. & Gayer, R.A. 1989: U-Pb ages of nepheline syenite pegmatites from the Seiland Magmatic Province, northern Norway. In Gayer, R.A. (ed.): *The Caledonide geology of Scandinavia*, Graham and Trotman, London, pp. 3–8. [https://doi.org/10.1007/978-94-009-2549-6\\_1](https://doi.org/10.1007/978-94-009-2549-6_1).
- Pfeifer, H.-R. 1977: A model for fluids in metamorphosed ultramafic rocks. Observations at surface and subsurface conditions (high pH spring waters). *Schweizerische Mineralogische Petrographische Mitteilungen* 57, 361–396.
- Raiswell, R. 1984: Chemical-Models of Solute Acquisition in Glacial Melt Waters. *Journal of Glaciology* 30, 49–57. <https://doi.org/10.1017/S0022143000008480>.
- Rao, M.N., Sutton, S.R., McKay, D.S. & Dreibus, G. 2005: Clues to Martian brines based on halogens in salts from nakhlites and MER samples. *Journal of Geophysical Research* 110, E12S06. <https://doi.org/10.1029/2005JE002470>.
- Roberts, D. 1973: Geologisk kart over Norge, berggrunnskart Hammerfest, scale 1:250,000, *Norges geologiske undersøkelse*, description in NGU 301 by David Roberts.
- Roberts, D. 2003: The Scandinavian Caledonides: event chronology, palaeogeographic settings and likely modern analogues. *Tectonophysics* 365, 283–299.
- Roberts, R.J. 2007: *The Seiland Igneous Province, Northern Norway: Age, Provenance, and Tectonic Significance*. Ph.D. thesis, University of the Witwatersrand, Johannesburg, 223 pp.
- Roberts, R.J., Corfu, F., Torsvik, T.H., Ashwal, L.D. & Ramsay, D.M. 2006: Shortlived mafic magmatism at 560–570 Ma in the northern Norwegian Caledonides: U–Pb zircon ages from the Seiland Igneous Province. *Geological Magazine* 143, 887–903. <https://doi.org/10.1017/S0016756806002512>.
- Roberts, R.J., Corfu, F., Torsvik, T.H., Hetherington, C.J. & Ashwal, L.D. 2010: Age of alkaline rocks in the Seiland Igneous Province. *Journal of the Geological Society* 167, 71–81. <https://doi.org/10.1144/0016-76492009-014>.
- Robins, B. 1971: The plutonic geology of the Caledonian complex of Southern Seiland, Northern Norway. PhD thesis, University of Leeds, 278 pp.
- Robins, B. 1972: Syenite-carbonatite relationships in the Seiland gabbro province, Finnmark, Northern Norway. *Norges geologiske undersøkelse* 272, 43–58.
- Robins, B. 1996: The Seiland Igneous Province, North Norway: General geology and magmatic evolution. In NGU: *The Seiland Igneous Province, North Norway. Field trip guidebook*, IGCP project 336. NGU Report 96.127, 34 pp.
- Robins, B. & Gardner, P.M. 1975: The magmatic evolution of the Seiland province, and Caledonian plate boundaries in Northern Norway. *Earth and Planetary science letters* 26, 167–178. [https://doi.org/10.1016/0012-821X\(75\)90084-9](https://doi.org/10.1016/0012-821X(75)90084-9).
- Robins, B. & Tysseland, M. 1983: The geology, geochemistry and origin of ultrabasic fenites associated with the Pollen carbonatite, Finnmark, Norway. *Chemical Geology* 40, 65–95. [https://doi.org/10.1016/0009-2541\(83\)90092-X](https://doi.org/10.1016/0009-2541(83)90092-X).
- Siedlecka, A., Roberts, D., Nystuen, J.P. & Olavyanishnikov, V.G. 2004: Northeastern and northwestern margins of Baltica in Neoproterozoic time: evidence from the Timanian and Caledonian orogens. Geological Society of London, *Memoirs* 30, 169–190.
- Skogen, J.H. 1980: *Lillebukt alkaline kompleks: Karbonatittens indre strukturer og dens metamorfe og tektoniske utvikling*. Cand. real. thesis, University of Bergen, 170 pp.
- Stober, I. 1995: *Die Wasserführung des kristallinen Grundgebirges*. Ferdinand Enke Verlag, Stuttgart, 191 pp.

- Stober, I. & Bucher, K. 1999a: Origin of salinity of deep groundwater in crystalline rocks. *Terra Nova* 11, 181–185.  
<https://doi.org/10.1046/j.1365-3121.1999.00241.x>.
- Stober, I. & Bucher, K. 1999b: Deep Groundwater in the crystalline basement of the Black Forest region. *Applied Geochemistry* 14, 237–254. [https://doi.org/10.1016/S0883-2927\(98\)00045-6](https://doi.org/10.1016/S0883-2927(98)00045-6).
- Stober, I., Richter, A., Brost, E. & Bucher, K. 1999: The Ohlsbach Plume: Natural Release of Deep Saline Water from the Crystalline Basement of the Black Forest. *Hydrogeology Journal* 7, 273–283.  
<https://doi.org/10.1007/s100400050201>.
- Stober, I., Zhu, Y. & Bucher, K. 2002: Water-rock reactions in a barite-fluorite underground mine, Black Forest (Germany). In Stober, I. & Bucher, K. (eds.): *Water Rock Interaction, Water Science and Technology Library* 40, Kluwer Academic Publishers, Dordrecht, pp. 171–188. [https://doi.org/10.1007/978-94-010-0438-1\\_7](https://doi.org/10.1007/978-94-010-0438-1_7).
- Strand, T. 1951: Biotitt-søvitt på Stjernøy. *Norges geologiske undersøkelse* 183, 10–19.
- Strand, T. 1981: *Lillebukt alkaline kompleks: karbonatittens mineralogi og petrokjemi*. Cand. real. thesis, University of Bergen, 249 pp.
- Sturt, B.A. & Ramsay, D.M. 1965: The alkaline complex of the Breivikbotn area, Sørøy, Northern Norway. *Norges geologiske undersøkelse* 231, 1–142.
- Tegner, C., Robins, B., Reginiussen, H. & Grundvig, S. 1999: Assimilation of crustal xenoliths in a basaltic magma chamber: Sr and Nd isotopic constraints from the Hasvik layered intrusion, Norway. *Journal of Petrology* 40, 363–380.  
<https://doi.org/10.1093/petroj/40.3.363>.
- Teiber, H. 2010: *The Chemical Composition of Surface Waters from the Seiland Igneous Province, Northern Norway*. MSc thesis, University of Freiburg, 142 pp.
- Torsvik, T.H., Smethurst, M.A., Meert, J.G., van der Voo, R., McKerrow, W.S., Brasier, M.D., Sturt, B.A. & Walderhaug, H.J. 1996: Continental breakup and collision in the Neoproterozoic and Palaeozoic: A tale of Baltica and Laurentia. *Earth Science Reviews* 40, 229–258.  
[https://doi.org/10.1016/0012-8252\(96\)00008-6](https://doi.org/10.1016/0012-8252(96)00008-6).
- Tranter, M., Brown, G.H., Raiswell, R., Sharp, M. & Gurnell, A. 1993: A Conceptual-Model of Solute Acquisition by Alpine Glacial Meltwaters. *Journal of Glaciology* 39, 573–581.  
<https://doi.org/10.1017/S0022143000016464>.
- Venturelli, G., Contini, S., Bonazzi, A. & Mangea, A. 1997: Weathering of ultramafic rocks and element mobility at Mt. Prinzera, Northern Apennines, Italy. *Mineralogical Magazine* 61, 765–778.  
<https://doi.org/10.1180/minmag.1997.061.409.02>.
- Woolley, A.R. & Kempe, D.R.C. 1989: Carbonatites: nomenclature, average chemical composition, and element distribution. In Bell, K. (ed.): *Carbonatites: genesis and evolution*, Unwin Hyman, London, pp. 1–13.
- Zakharova, E.A., Pokrovsky, O.S., Dupré, B., Gaillardet, J. & Efimova, L.E. 2007: Chemical weathering of silicate rocks in Karelia region and Kola peninsula, NW Russia: Assessing the effect of rock composition, wetlands and vegetation. *Chemical Geology* 242, 255–277.  
<https://doi.org/10.1016/j.chemgeo.2007.03.018>.
- Zedef, V., Russell, M.J. & Fallick, A.E. 2000: Genesis of vein stockwork and sedimentary magnesite and hydromagnesite deposits in the ultramafic terranes of southwestern Turkey: a stable isotope study. *Economic Geology* 95, 429–446.  
<https://doi.org/10.2113/gsecongeo.95.2.429>.
- Zhou, W. 2010: *Chemical evolution at surface condition in the Zermatt-Saas area (Swiss Alps): A geo-hydrochemistry study on surface water-rock interaction*. PhD thesis, University of Freiburg, 176 pp.